Supporting Information for

Compression and thermal expansion in organic and metal-organic crystals: the pressure-temperature correspondence rule

Michał Kaźmierczak, Ewa Patyk-Kaźmierczak and Andrzej Katrusiak*

Faculty of Chemistry, Adam Mickiewicz University in Poznań, Uniwersytetu Poznańskiego 8, Poznań 61-614 Poland

S1. Experimental details

S1.1. Statistical data analysis

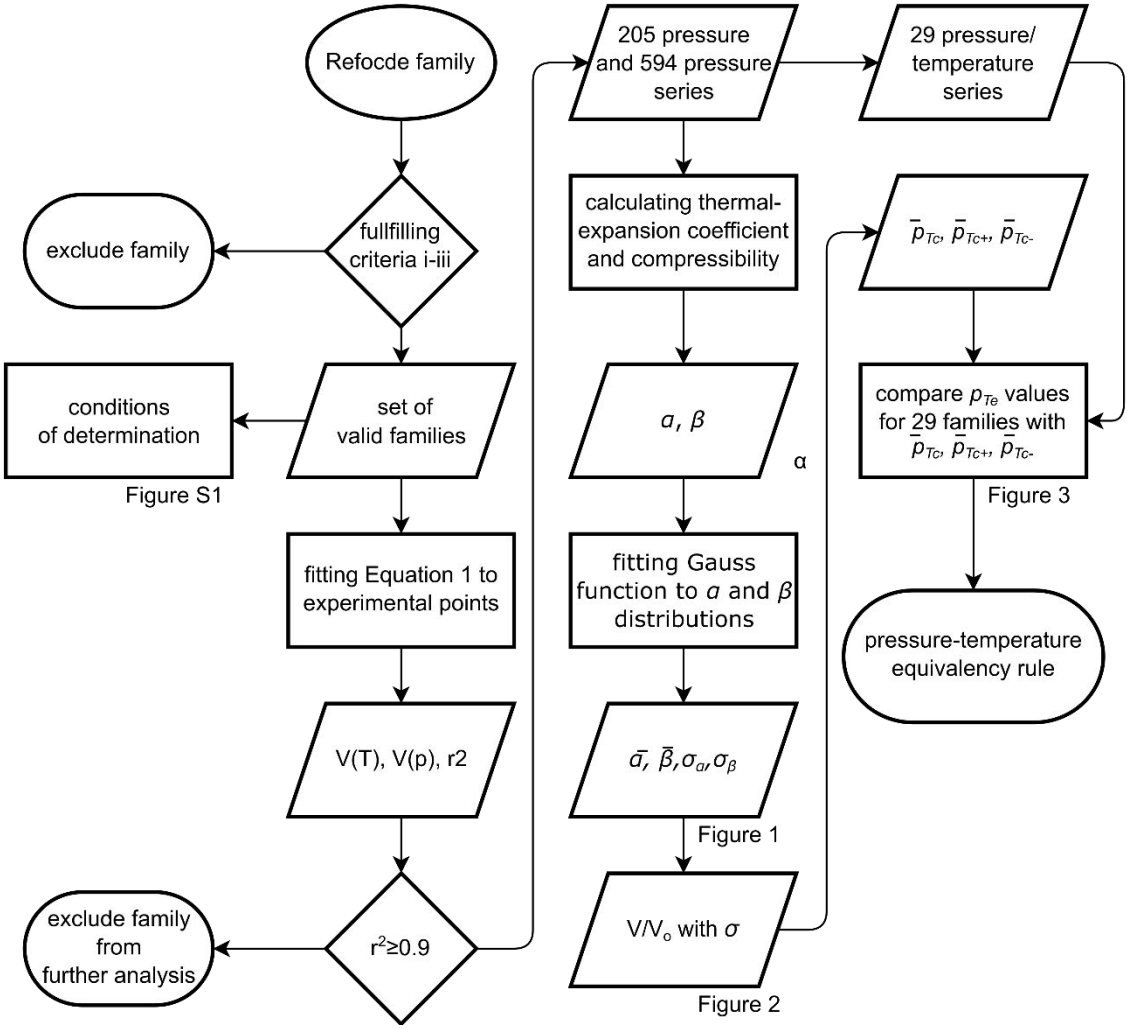

Scheme S1 Flow chart representing steps in the data analysis leading to formulation of the pressure-temperature-equivalency rule.

S1.2. Crystal structures analysis

For the analysis of crystal structures of 29 refcode families investigated in this work fallowing criteria were used:

- Structures determined at ambient conditions were considered (specific refcodes listed in Table S1).
- In order to establish the dimensionality of the intermolecular interaction pattern, all contacts shorter than the sum of van der Waals radii and with D-H···A angle higher than 110° were taken under the consideration.
- Following dimensionality types were assigned
    - 0D: no H-bonds were present or they bonded molecules into finite arrangement,
    - 1D: molecules form H-bonded chains,
    - 2D: molecules form H-bonded sheets,
    - 3D: molecules are H-bonded into 3 dimentional framework.
- Both, structural voids volume and intermolecular contacts, were calculated using program Mercury.[1]

S2. Tables

Table S1 Values of parameters $\overline{p}_{Tc}$, $\overline{p}_{Tc-}$ and $\overline{p}_{Tc+}$ for the temperature decrease from 300 K to temperature T_1.

T_1 [K]	$\overline{p}_{Tc}$ [GPa]	$\overline{p}_{Tc-}$ [GPa]	$\overline{p}_{Tc+}$ [GPa]
250	0.122	0.055	0.331
200	0.233	0.097	0.622
150	0.348	0.141	0.925
100	0.467	0.185	1.243

Table S2 Selected chemical and crystallographic information for 29 series of structures that were studied at varied temperature and pressure, and fulfilled criteria described in the experimental section of the manuscript.

Refcode family	Chemical name	Formula	Polymorph[a]	Crystal type	Space group	Dimen-sionality[b]	Voids volume [%][c]	Types of H-bonds[d]	Ambient conditions refcode
BCBANN	syn-1,6:8,13-bis-carbonyl[14]annulene	$C_{16}H_{10}O_2$	-	Mol.[e]	$P\,2_1/n$	1D	15.6	C-H···O	BCBANN07
BEMSAO	catena-(bis(μ$_2$-2-(1-Methylpyrazol-4-yl)-4,4,5,5-tetramethylimidazoline-3-oxide-1-oxyl-N',O)-tetrakis(hexafluoroacetylacetonato-O,O')-di-copper(II)	$[C_{42}H_{38}Cu_2F_{24}N_8O_{12}]_n$	Triclinic	CP	$P\,\bar{1}$	1D	23.4	C-H···O C-H···F	BEMSAO11
BIHXIC	pyrazinium tetrachloro-gold(III)	$C_4H_5N_2^+$, $AuCl_4^-$	-	Ionic	$P\,4_2/ncm$	3D	16.4	C-H···Cl	BIHXIC06
BOLDIP	guanidinium perchlorate	$CH_6N_3^+$, ClO_4^-	-	Ionic	$R\,3$	2D	15.2	N-H···O	BOLDIP13
CABCUD	1-(4-Methylphenylsulfonyl)-3-(hexahydro-1H-azepin-1-yl)-urea	$C_{14}H_{21}N_3O_3S$	I	Mol.	$P\,\bar{1}$	1D	15.2	N-H···O	CABCUD26
CABCUD	1-(4-Methylphenylsulfonyl)-3-(hexahydro-1H-azepin-1-yl)-urea	$C_{14}H_{21}N_3O_3S$	II	Mol.	$P\,\bar{1}$	2D	17.3	C-H···O N-H···O	CABCUD35
CEGFEA	catena-(bis(μ$_2$-2-Methylimidazolato)-di-silver(I)	$[C_8H_{10}Ag_2N_4]_n$	-	CP[e]	$P\,2_1/n$	1D	16.7	-	CEGFEA02
COXZAS	6-hydroxy-4,5-dimethyl-2-phenylpyridazin-3(2H)-one	$C_{12}H_{12}N_2O_2$	α	Mol.	$C\,2/c$	3D	19.3	C-H···O O-H···O	COXZAS28
DANTEN	9,9'-bianthrylidene-10,10'-dione	$C_{28}H_{16}O_2$	Yellow	Mol.	$P\,2_1/c$	3D	19.5	C-H···O	DANTEN04
IBPRAC	2-(4-Isobutylphenyl)propionic acid	$C_{13}H_{18}O_2$	I	Mol.	$P\,2_1/c$	1D	23.2	C-H···O O-H···O	IBPRAC06
IMEGIR	DL-alaninium semioxalate monohydrate	$C_3H_8NO_2^+$, $C_2HO_4^-$, H_2O	-	Ionic	$P\,2_1/c$	3D	12.8	C-H···O O-H···O N-H···O	IMEGIR
MAGVOG	catena-((μ$_2$-Ethylene-1,2-diamine-N,N')-silver(I) nitrate)	$[C_2H_8AgN_2^+]_n$,n(NO_3^-)	I	CP	$C\,2/c$	3D	7.0	C-H···O N-H···O	MAGVOG34
MCBZIM	1,3-dihydro-2H-benzimidazole-2-thione	$C_7H_6N_2S$	-	Mol.	$P\,2_1/m$	1D	18.1	N-H···S	MCBZIM13
MUTKUH	tris(μ$_2$-Pyrazolato-N,N')-tri-gold(I)	$C_9H_9Au_3N_6$	-	Mol.	$P\,2_1/c$	2D	18.2	-	MUTKUH13

[a] Where applicable; [b] dimensionality of coordination polymer or of the crystal lattice formed *via* intermolecular contacts (for ionic and molecular crystals) at ambient conditions; [c] molecular voids volume calculated with Mercury program for contact surface with probe radius and grid spacing of 0.5 and 0.1 Å, respectively; [d] Types of hydrogen bonds present in crystal structure at ambient conditions according to criteria listed in section S1.2 [e] Mol.- molecular crystal, CP-coordination polymer;

Table S2 *Continuation.*

Refcode family	Chemical name	Formula	Polymorph[a]	Crystal type	Space group	Dimen-sionality[c]	Voids volume [%][d]	Types of H-bonds	Ambient conditions refcode
NALCYS	N-acetyl-L-cysteine	$C_5H_9NO_3S$	I	Mol.	*P* 1	3D	11.5	O-H···O S-H···O N-H···S	NALCYS11
NAPHTA	naphthalene	$C_{10}H_8$	-	Mol.	*P* 2_1/*a*	2D	12.6	-	NAPHTA36
NONWES	dichloro-(1,4,7-oxadithionane)-palladium(II)	$C_6H_{12}Cl_2OPdS_2$	*γ*	Mol.	*P* 2_1/*n*	3D	14.4	C-H···Cl	NONWES47
OBUQUZ	2-phenyl-1H-imidazole	$C_9H_8N_2$	-	Mol.	*A ma*2	1D	17.4	-	OBUQUZ03
PCYPOL	4-hydroxybenzonitrile	C_7H_5NO	*Pbcn*	Mol.	*P bcn*	3D	21.9	C-H···O O-H···N C-H···N	PCYPOL11
PESBAT	4-cyano-1-methylpyridin-1-ium 5,6-dichloro-2,3-dicyanosemiquinone radical anion	$C_7H_7N_2^+$, $C_8Cl_2N_2O_2^-$	-	Mol.	*P* 2_1/*n*	3D	11.0	C-H···O C-H···N	PESBAT12
PEQXOY	6-azido-1,2,3,4-tetrazolo[1,5-b]pyridazine	$C_4H_2N_8$	*α*	Mol.	*P nma*	1D	19.0	C-H···N	PEQXOY12
PYRZOL	pyrazole	$C_3H_4N_2$	*α*	Mol.	*P* 2_1*cn*	1D	21.6	N-H···N	PYRZOL08
QQQAUG	6-chloro-4H-1,2,4-benzothiadiazine-7-sulfonamide 1,1-dioxide	$C_7H_6ClN_3O_4S_2$	I	Mol.	*P* 1	3D	15.3	C-H···O N-H···O N-H···N	QQQAUG09
SAZZID	bis(4-chloropyridinium) tetrachloro-cobalt(II)	$2(C_5H_5ClN^+)$, Cl_4Co^{2-}	-	Ionic	*C* 2/*c*	3D	20.7	C-H···Cl N-H···Cl	SAZZID01
SEHHIX	bis(4-chloropyridinium) tetrabromo-cobalt(II)	$2(C_5H_5ClN^+)$, Br_4Co^{2-}	-	Ionic	*C* 2/*c*	3D	22.0	C-H···Br N-H···Br	SEHHIX01
WEMWEQ	2-(trimethylamino)acetic acid /betaine	$C_5H_{11}NO_2$	-	Ionic	*P nma*	3D	10.0	C-H···O	WEMWEQ01
WEYQAU	catena-(1-Ethyl-3-methylimidazol-3-ium (μ_4-benzene-1,3,5-tricarboxylato)-manganese)	$[C_9H_3MnO_6^-]_n$, $C_6H_{11}N_2^+$		CP	*P bca*	3D	9.5	C-H···O	WEYQAU03
YIHHON	N-Trideuteromethylammonioacetate	$C_3H_7NO_2$	-	Mol.	*P* $2_12_12_1$	3D	22.6	C-H···O N-H···O	YIHHON12
YOSRUU	tris(μ_2-3,4,5-Trimethylpyrazolato-N,N')-tri-gold(i)	$C_{18}H_{27}Au_3N_6$	-	Mol.	*P* 2_1/*c*	1D	21.9	-	YOSRUU08

Table S3 The p_{Tc} value and crystal behavior types for 29 structures analyzed in this work.

Refcode family	Chemical name	Polymorph[a]	Behaviour type	p_{Tc}[b] [GPa]	References	
					T	p
BCBANN	syn-1,6:8,13-bis-carbonyl[14]annulene	-	I	0.26	2	
BIHXIC	pyrazinium tetrachloro-gold(III)	-	I	0.23	3	
BOLDIP	guanidinium perchlorate	-	I	0.38	4	5
CABCUD	1-(4-methylphenylsulfonyl)-3-(hexahydro-1H-azepin-1-yl)-urea	I	I	0.40	6,7	
CABCUD	1-(4-methylphenylsulfonyl)-3-(hexahydro-1H-azepin-1-yl)-urea	II	I	0.16		
CEGFEA	catena-(bis(μ_2-2-methylimidazolato)-di-silver(I)	-	I	0.36	8	
COXZAS	6-hydroxy-4,5-dimethyl-2-phenylpyridazin-3(2H)-one	α	I	0.32	9	
DANTEN	9,9'-bianthrylidene-10,10'-dione	Yellow	I	0.26	10	11
IBPRAC	2-(4-isobutylphenyl)propionic acid	I	I	0.32	12	
IMEGIR	DL-alaninium semioxalate monohydrate	-	I	0.31	13	
MCBZIM	1,3-dihydro-2H-benzimidazole-2-thione	-	I	0.27	14	
MUTKUH	tris(μ_2-pyrazolato-N,N')-tri-gold(I)	-	I	0.25	15	
NALCYS	N-acetyl-L-cysteine	I	I	0.31	16	17
NAPHTA	naphthalene	-	I	0.42	18	19
NONWES	dichloro-(1,4,7-oxadithionane)-palladium(II)	γ	I	0.28	20	
OBUQUZ	2-phenyl-1H-imidazole	-	I	0.28	21	
PCYPOL	4-hydroxybenzonitrile	*Pbcn*	I	0.29	22	
PESBAT	4-cyano-1-methylpyridin-1-ium 5,6-dichloro-2,3-dicyanosemiquinone radical anion	-	I	0.50	23	
PYRZOL	pyrazole	α	I	0.40	24	
QQQAUG	6-chloro-4H-1,2,4-benzothiadiazine-7-sulfonamide 1,1-dioxide	I	I	0.22	25	26
YIHHON	N-trideuteromethylammonioacetate	-	I	0.16	27	28
BEMSAO	catena-(bis(μ_2-2-(1-methylpyrazol-4-yl)-4,4,5,5-tetramethylimidazoline-3-oxide-1-oxyl-N',O)-tetrakis(hexafluoroacetylacetonato-O,O')-di-copper(II)	Triclinic	II	0.16	29	
MAGVOG	catena-((μ_2-ethylene-1,2-diamine-N,N')-silver(I) nitrate)	I	II	0.54	30	
PEQXOY	6-azido-1,2,3,4-tetrazolo[1,5-b]pyridazine	α	II	0.41	31	
SAZZID	bis(4-chloropyridinium) tetrachloro-cobalt(II)	-	II	0.35	32	
SEHHIX	bis(4-chloropyridinium) tetrabromo-cobalt(II)	-	II	0.32		
WEMWEQ	2-(trimethylamino)acetic acid /betaine	-	II	0.38	27	28
WEYQAU	catena-(1-Ethyl-3-methylimidazol-3-ium (μ_4-benzene-1,3,5-tricarboxylato)-manganese)		II	0.20	33	34
YOSRUU	tris(μ_2-3,4,5-trimethylpyrazolato-N,N')-tri-gold(i)	-	II	0.24	15	

[a] Where applicable; [b]p_{Tc}- temperature-equivalent pressure i.e. pressure required to enforce same relative unit-cell volume change as lowering temperature from 300 to 100 K;

Table S4 List of refcodes for 29 series of structures that were studied at varied temperature and pressure, and fulfilled criteria described in the experimental section of the manuscript.

Family	Φ_T [°]	r_T	ΔT [K]	$r_T/\Delta T \cdot 10^{-5}$ [K^{-1}]	Φ_p [°]	r_p	Δp [GPa]	$r_p/\Delta p \cdot 10^{-5}$ [GPa^{-1}]
BCBANN	49.97	0.0032	-203.00	1.58	25.30	0.0219	9.50	230.71
BIHXIC	60.00	0.0001	-166.00	0.06	60.00	0.0001	12.67	1.01
BOLDIP	60.00	0.0124	-275.00	4.51	60.00	0.0169	1.35	1254.44
CABCUD1	232.23	0.0010	-195.00	0.51	228.25	0.0095	5.64	167.87
CABCUD2	216.74	0.0108	-195.00	5.54	233.21	0.0187	6.50	288.15
CEGFEA	208.70	0.0090	-200.00	4.50	220.87	0.0382	6.40	597.24
COXZAS	238.38	0.0059	-230.00	2.57	230.60	0.0023	0.50	456.14
DANTEN	279.68	0.0104	-410.00	2.54	295.71	0.0412	6.50	634.41
IBPRAC	79.10	0.0043	-196.00	2.19	18.15	0.0068	4.00	169.89
IMEGIR	297.04	0.0056	-200.00	2.80	272.42	0.0229	5.10	449.37
MCBZIM	79.19	0.0064	-213.00	3.00	98.40	0.0182	2.58	705.98
MUTKUH	280.01	0.0019	-193.00	0.98	277.11	0.0173	7.80	222.21
NALCYS	298.11	0.0016	-195.00	0.82	268.35	0.0065	6.05	107.31
NAPHTA	193.74	0.0029	-147.00	1.97	194.85	0.0178	5.60	318.06
NONWES	306.54	0.0011	-191.00	0.58	313.11	0.0098	9.86	99.09
OBUQUZ	70.64	0.0153	-190.00	8.05	47.76	0.0215	1.57	1370.76
PCYPOL	272.23	0.0025	-180.00	1.39	249.10	0.0145	4.04	358.03
PESBAT	177.54	0.0065	-270.00	2.41	168.13	0.0270	6.00	449.32
PYRZOL	215.62	0.0107	-210.00	5.10	203.87	0.0102	0.42	2437.85
QQQAUG	333.49	0.0006	-120.00	0.50	308.23	0.0160	4.00	399.28
YIHHON	192.08	0.0078	-195.00	4.00	148.49	0.0222	3.68	604.24
BEMSAO	99.20	0.0134	-265.00	5.06	201.57	0.0357	0.30	11910.33
MAGVOG	131.81	0.0169	-240.00	7.04	356.15	0.0145	0.80	1809.50
PEQXOY	286.47	0.0061	-193.10	3.16	5.38	0.0127	2.33	546.65
SAZZID	32.79	0.0061	-270.00	2.26	340.85	0.0285	4.10	695.15
SEHHIX	23.97	0.0056	-270.00	2.07	342.19	0.0231	3.73	619.34
WEMWEQ	350.46	0.0042	-195.00	2.15	15.45	0.0119	3.30	360.42
WEYQAU	218.43	0.0100	-240.20	4.16	276.91	0.0253	4.00	631.35
YOSRUU	189.96	0.0054	-193.10	2.80	87.54	0.0214	5.18	412.92

S3. Figures

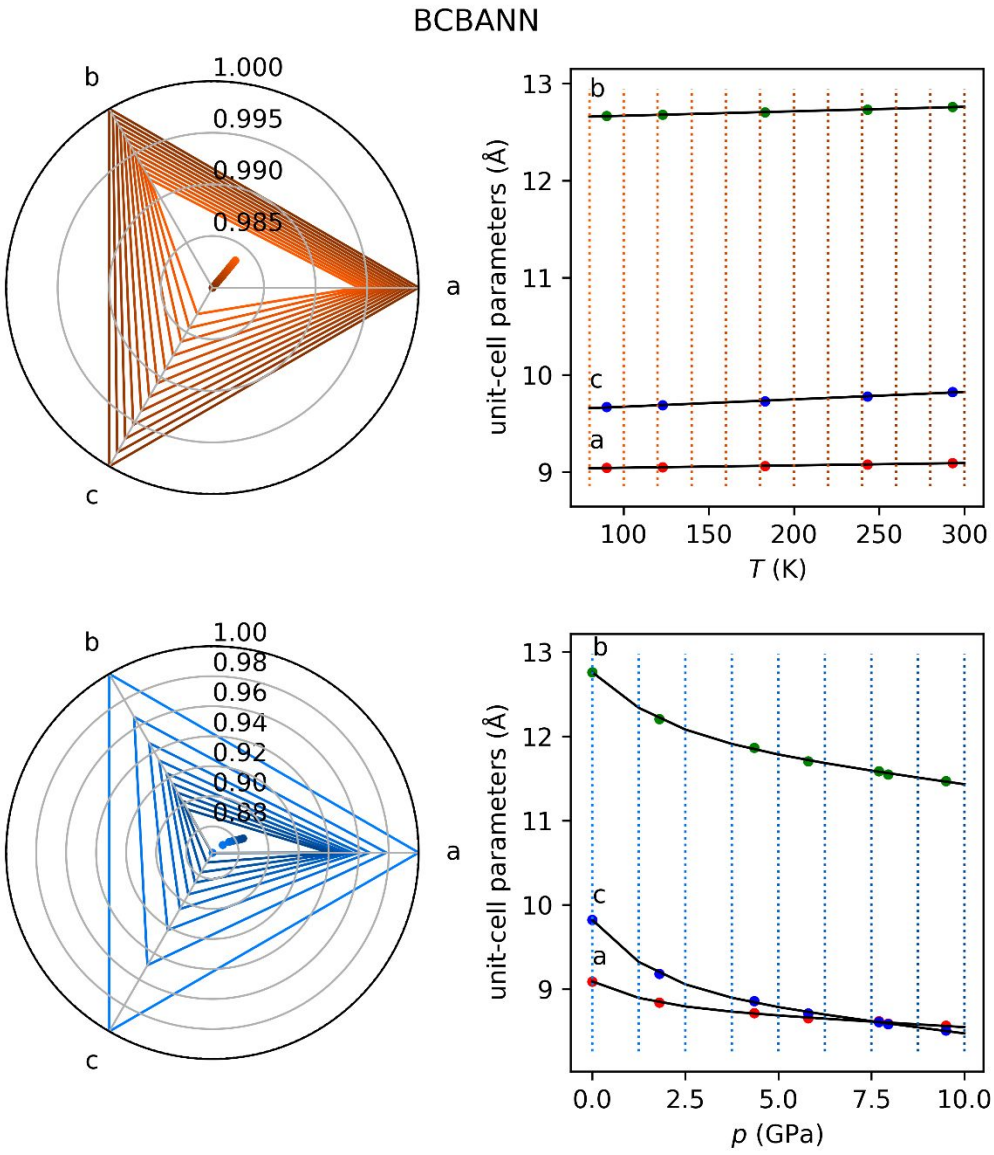

Figure S1. Change of unit-cell parameters lengths for syn-1,6:8,13-bis-carbonyl[14]annulene (refcode family:BCBANN[2]) in temperature (90-293 K) and pressure (ambient-9.5 GPa) range (right), as well as relative changes (left) calculated for selected pressure and temperature points (marked with blue and red dotted lines in pressure and temperature graphs on the right). Regression line was fitted to all experimental points to enable calculation of relative change of unit-cell parameters for any pressure and temperature conditions. The centroids of triangles are presented as dots of matching colors.

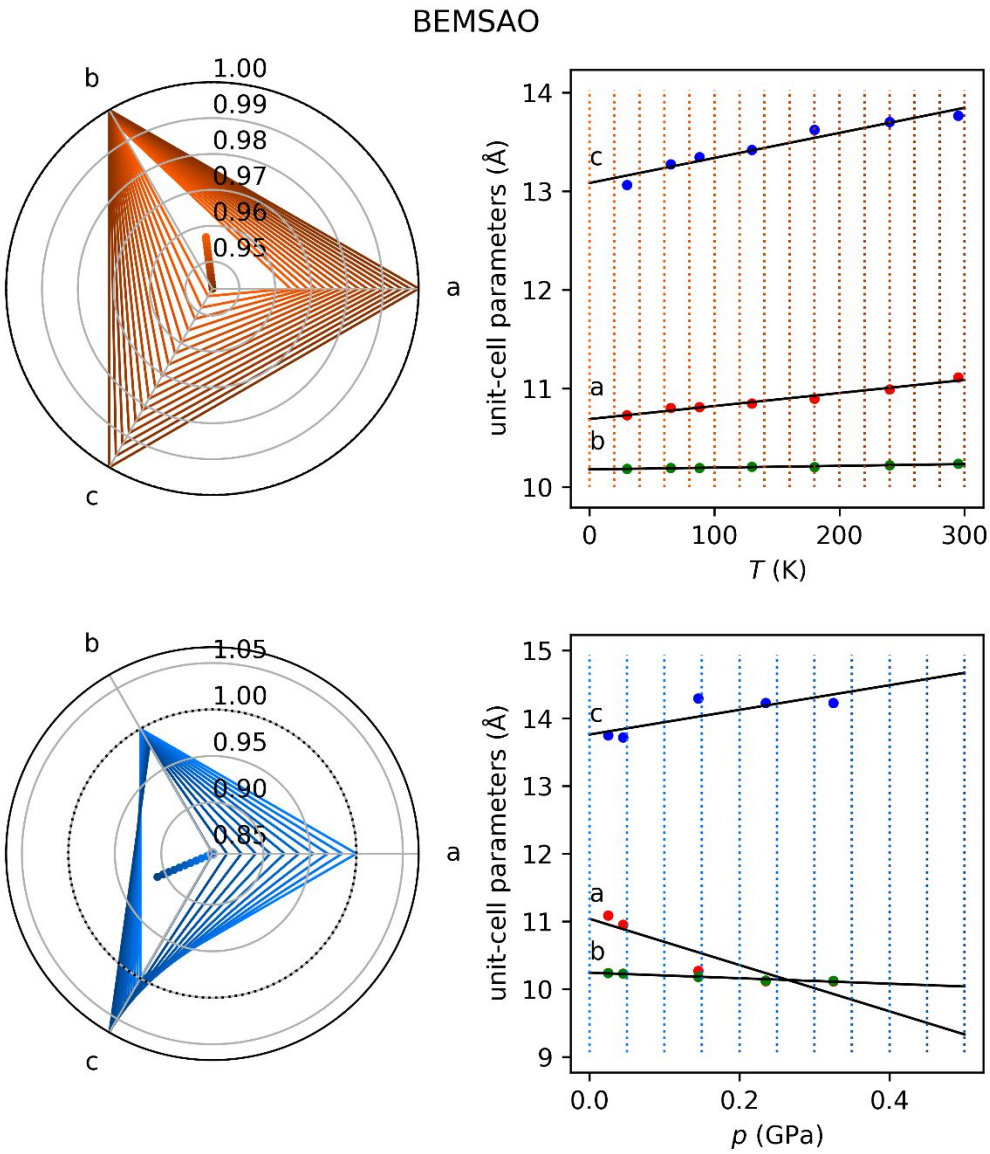

Figure S2. Change of unit-cell parameters lengths for catena-(bis(μ_2-2-(1-Methylpyrazol-4-yl)-4,4,5,5-tetramethylimidazoline-3-oxide-1-oxyl-N',O)-tetrakis(hexafluoroacetylacetonato-O,O')-di-copper(II)) triclinic polymorph (refcode family:BEMSAO[24]) in temperature (30-295 K) and pressure (0.02-0.32 GPa) range (right), as well as relative changes (left) calculated for selected pressure and temperature points (marked with blue and red dotted lines in pressure and temperature graphs on the right). Regression line was fitted to all experimental points to enable calculation of relative change of unit-cell parameters for any pressure and temperature conditions. The centroids of triangles are presented as dots of matching colors.

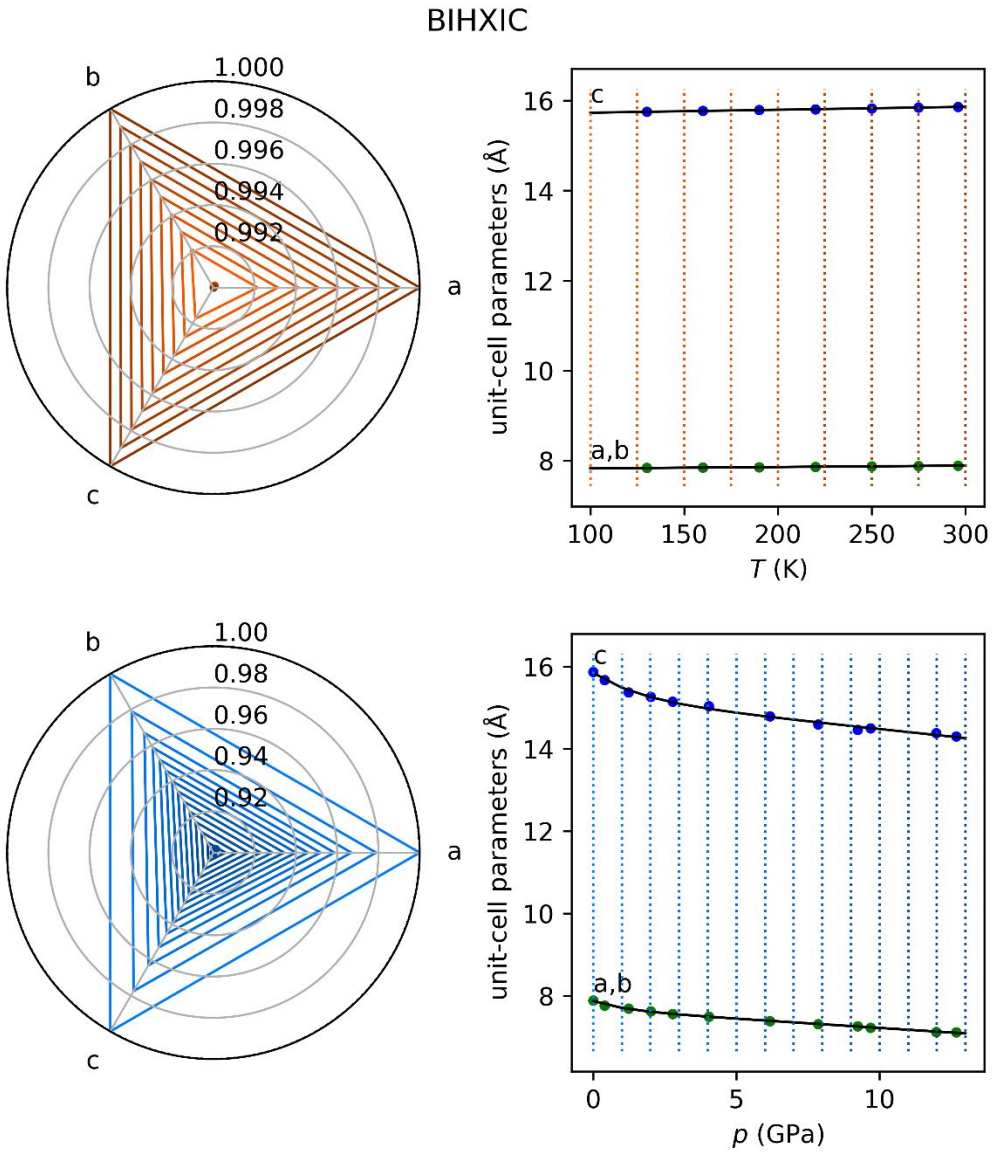

Figure S3. Change of unit-cell parameters lengths for pyrazinium tetrachloro-gold(III) (refcode family:BIHXIC[3]) in temperature (130-296 K) and pressure (ambient-12.675 GPa) range (right), as well as relative changes (left) calculated for selected pressure and temperature points (marked with blue and red dotted lines in pressure and temperature graphs on the right). Regression line was fitted to all experimental points to enable calculation of relative change of unit-cell parameters for any pressure and temperature conditions. The centroids of triangles are presented as dots of matching colors.

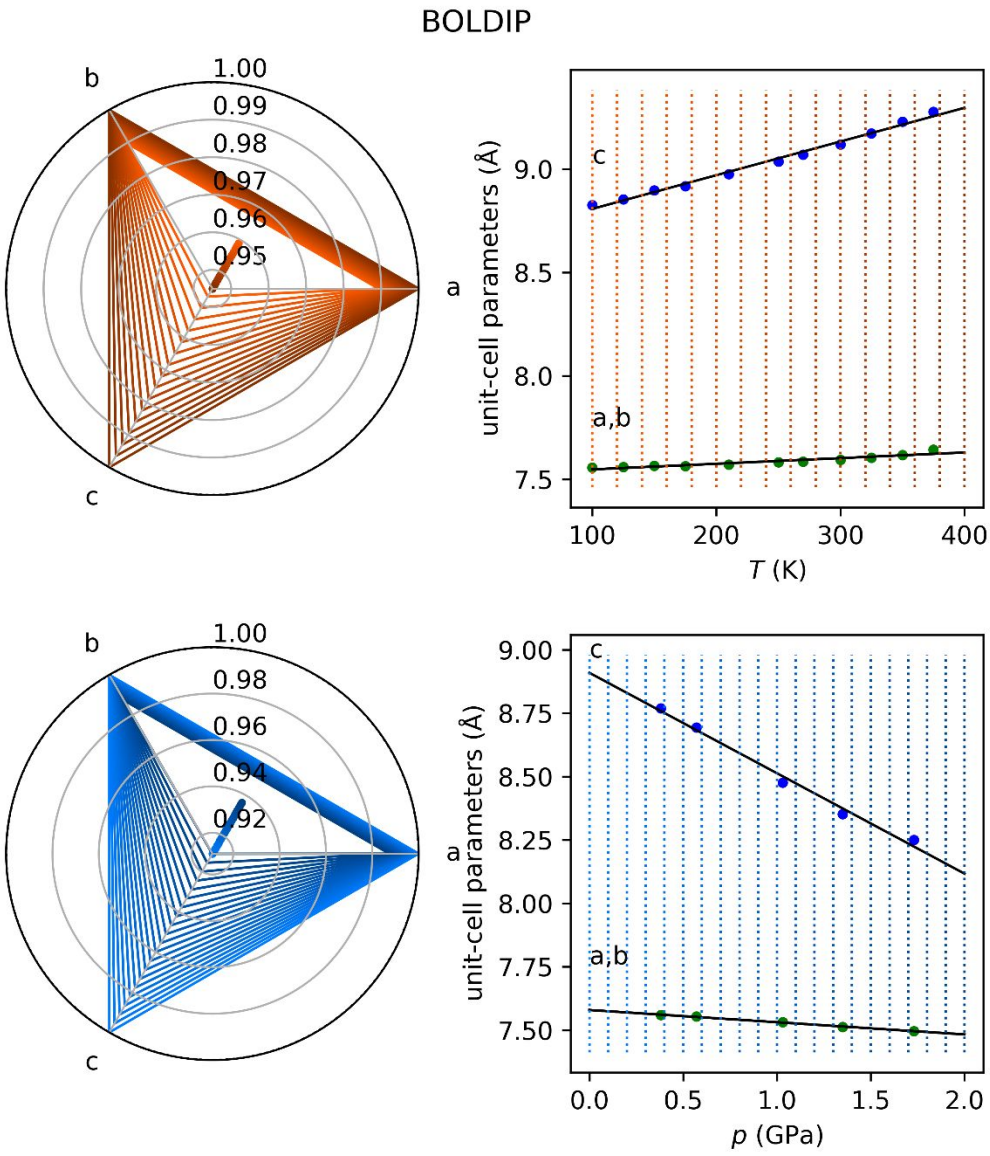

Figure S4. Change of unit-cell parameters lengths for guanidinium perchlorate (refcode family:BOLDIP) in temperature (100-375 K)[4] and pressure (0.38-1.73 GPa)[5] range (right), as well as relative changes (left) calculated for selected pressure and temperature points (marked with blue and red dotted lines in pressure and temperature graphs on the right). Regression line was fitted to all experimental points to enable calculation of relative change of unit-cell parameters for any pressure and temperature conditions. The centroids of triangles are presented as dots of matching colors.

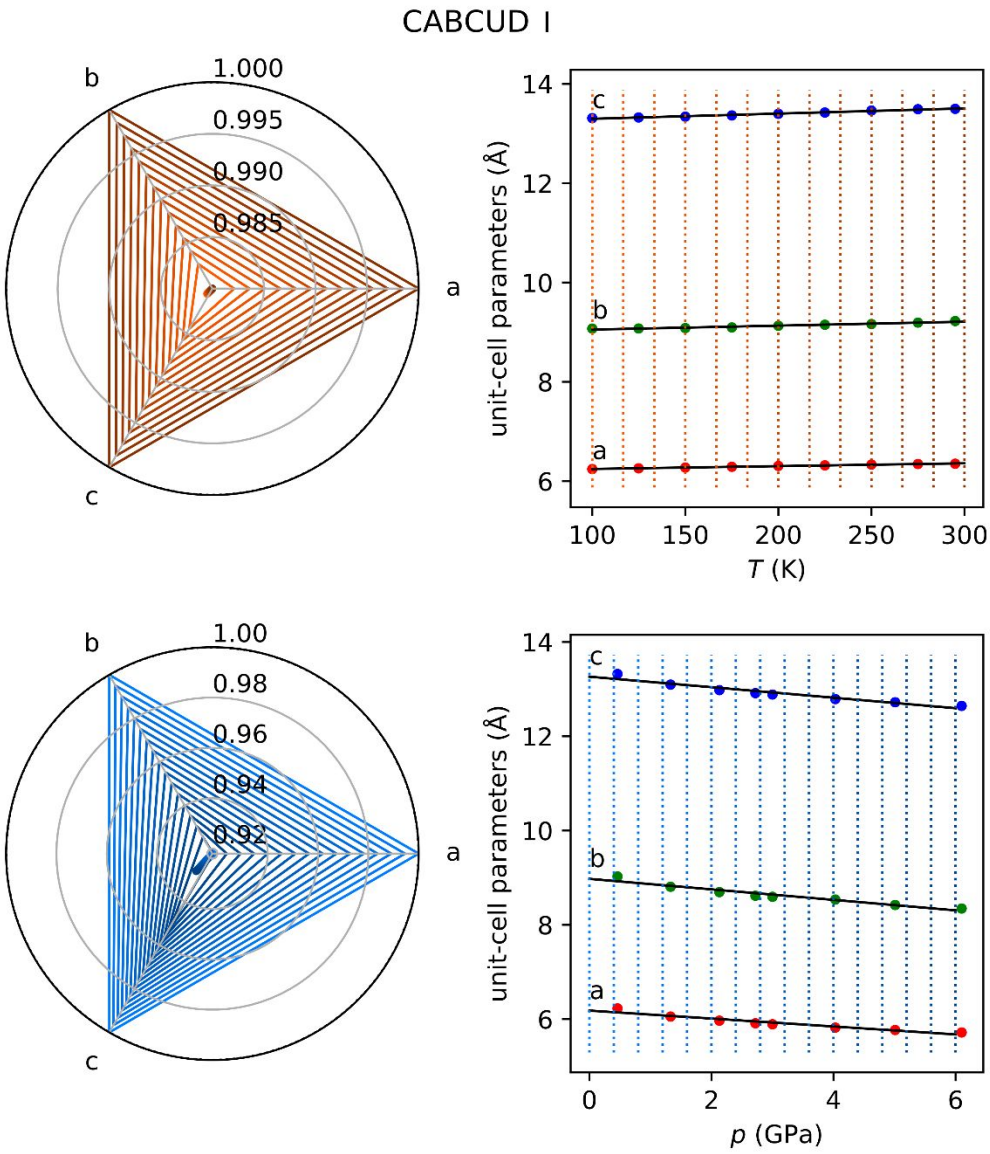

Figure S5. Change of unit-cell parameters lengths for 1-(4-Methylphenylsulfonyl)-3-(hexahydro-1H-azepin-1-yl)-urea polymorph I (refcode family:CABCUD[6,7]) in temperature (100-295 K) and pressure (0.46-6.10 GPa) range (right), as well as relative changes (left) calculated for selected pressure and temperature points (marked with blue and red dotted lines in pressure and temperature graphs on the right). Regression line was fitted to all experimental points to enable calculation of relative change of unit-cell parameters for any pressure and temperature conditions. The centroids of triangles are presented as dots of matching colors.

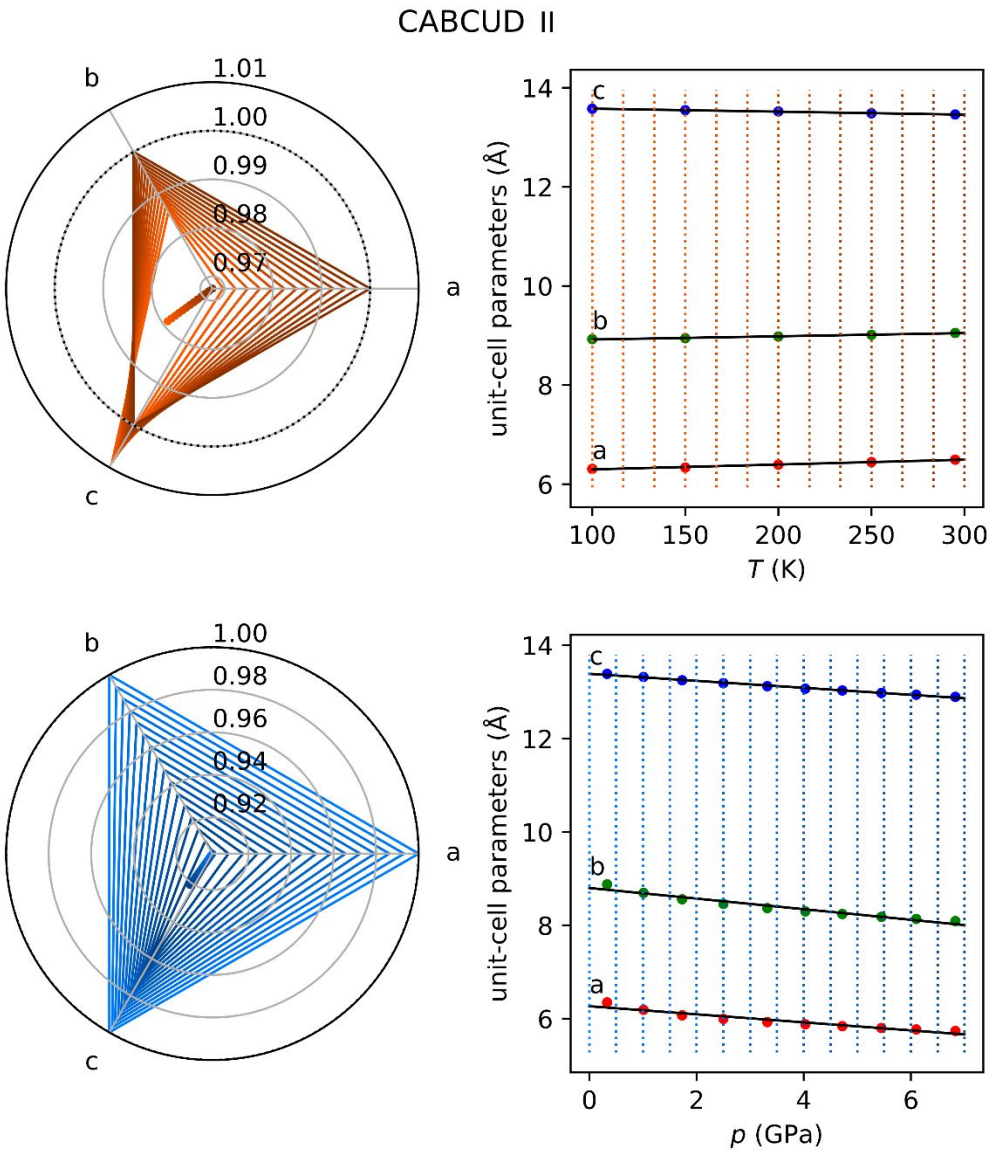

Figure S6. Change of unit-cell parameters lengths for 1-(4-Methylphenylsulfonyl)-3-(hexahydro-1H-azepin-1-yl)-urea polymorph II (refcode family:CABCUD[6,7]) in temperature (100-295 K) and pressure (0.33-6.83 GPa) range (right), as well as relative changes (left) calculated for selected pressure and temperature points (marked with blue and red dotted lines in pressure and temperature graphs on the right). Regression line was fitted to all experimental points to enable calculation of relative change of unit-cell parameters for any pressure and temperature conditions. The centroids of triangles are presented as dots of matching colors.

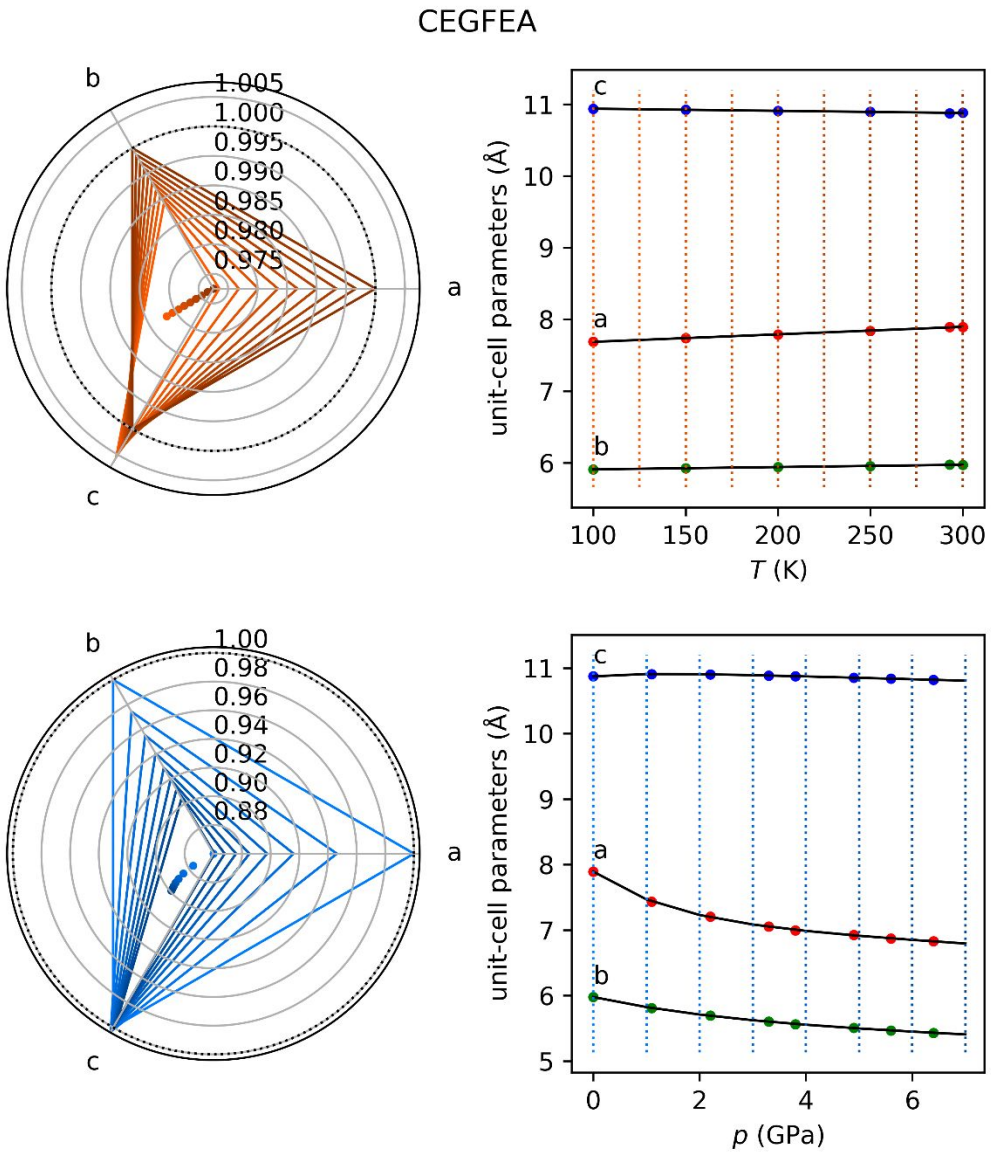

Figure S7. Change of unit-cell parameters lengths for catena-(bis(μ_2-2-Methylimidazolato)-di-silver(I)) (refcode family:CEGFEA[8]) in temperature (100-300 K) and pressure (ambient-6.4 GPa) range (right), as well as relative changes (left) calculated for selected pressure and temperature points (marked with blue and red dotted lines in pressure and temperature graphs on the right). Regression line was fitted to all experimental points to enable calculation of relative change of unit-cell parameters for any pressure and temperature conditions. The centroids of triangles are presented as dots of matching colors.

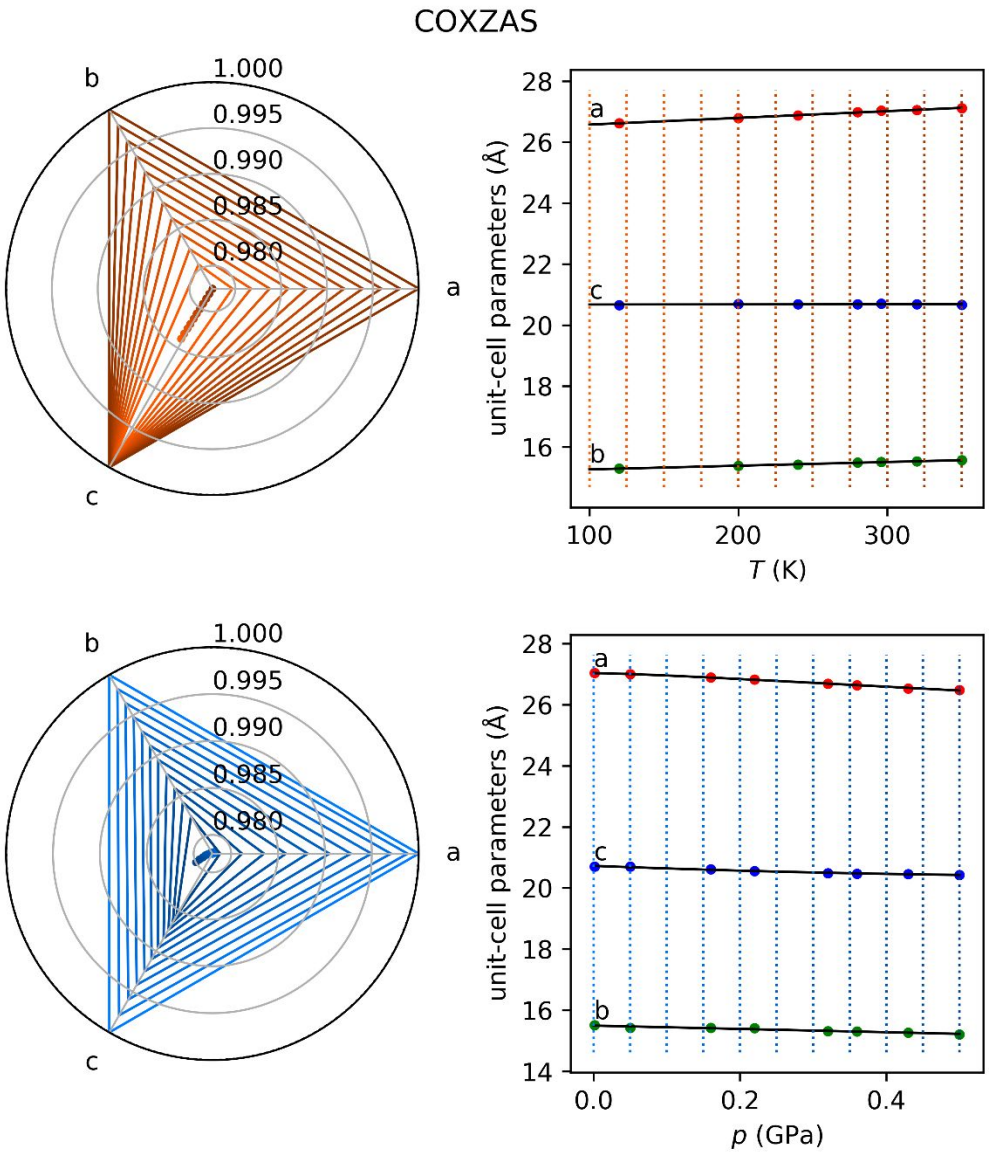

Figure S8. Change of unit-cell parameters lengths for 6-hydroxy-4,5-dimethyl-2-phenylpyridazin-3(2H)-one polymorph α (refcode family:COXZAS[9]) in temperature (120-350 K) and pressure (ambient-0.5 GPa) range (right), as well as relative changes (left) calculated for selected pressure and temperature points (marked with blue and red dotted lines in pressure and temperature graphs on the right). Regression line was fitted to all experimental points to enable calculation of relative change of unit-cell parameters for any pressure and temperature conditions. The centroids of triangles are presented as dots of matching colors.

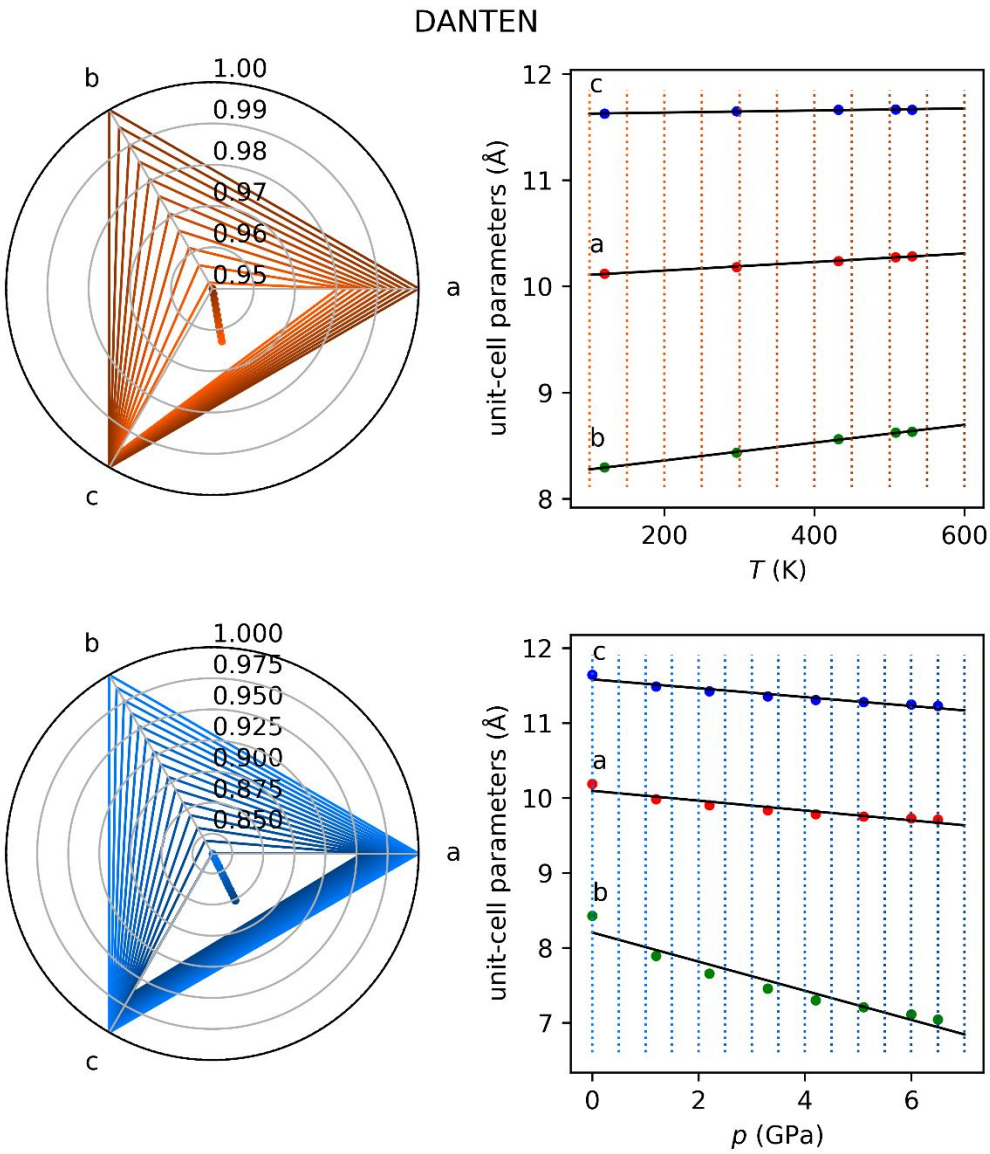

Figure S9. Change of unit-cell parameters lengths for 9,9'-bianthrylidene-10,10'-dione yellow polymorph (refcode family: DANTEN) in temperature (120-530 K)[10] and pressure (ambient-6.5 GPa)[11] range (right), as well as relative changes (left) calculated for selected pressure and temperature points (marked with blue and red dotted lines in pressure and temperature graphs on the right). Regression line was fitted to all experimental points to enable calculation of relative change of unit-cell parameters for any pressure and temperature conditions. The centroids of triangles are presented as dots of matching colors.

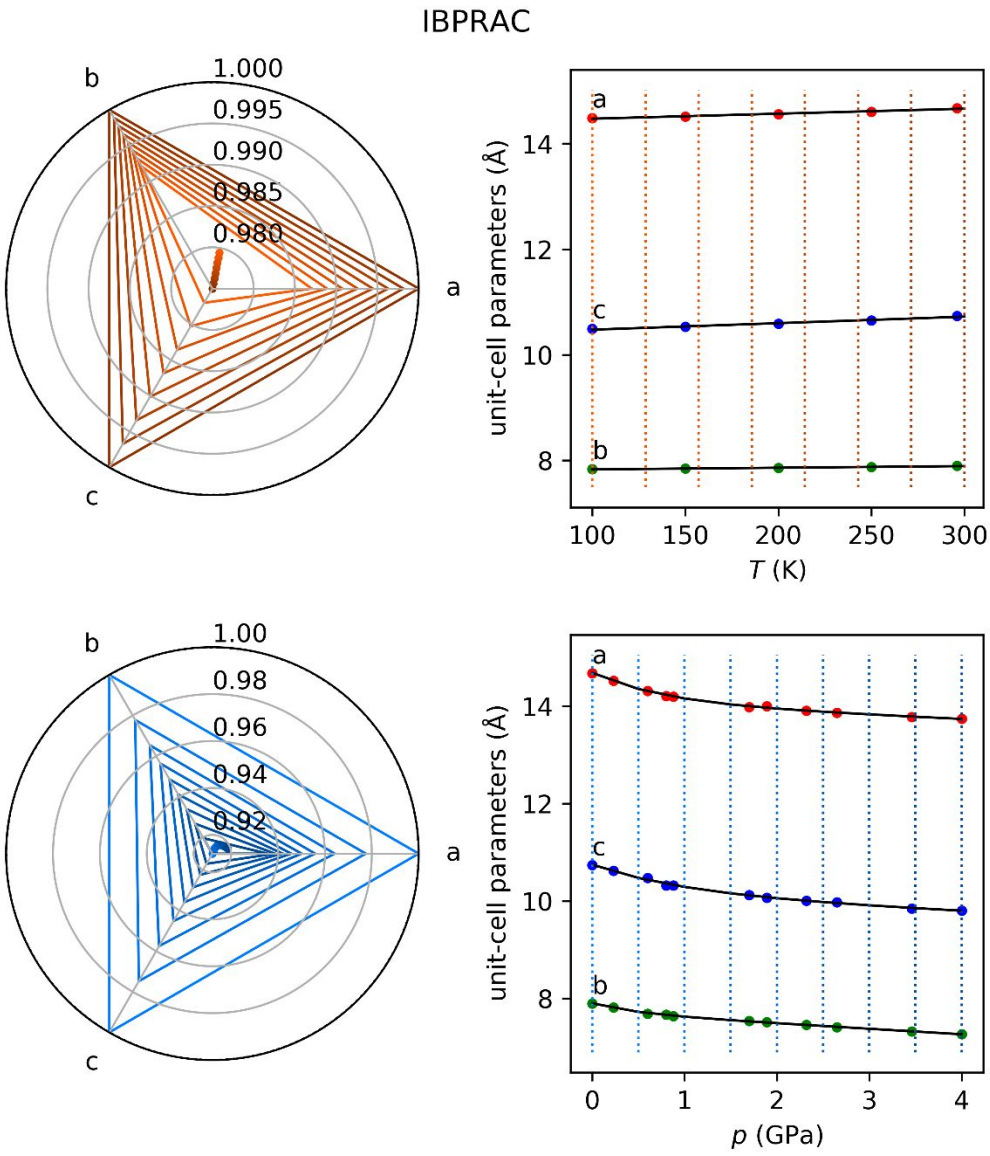

Figure S10. Change of unit-cell parameters lengths for 2-(4-Isobutylphenyl)propionic acid polymorph I (ibuprofen; refcode family:IBPRAC[12]) in temperature (100-296 K) and pressure (ambient-4 GPa) range (right), as well as relative changes (left) calculated for selected pressure and temperature points (marked with blue and red dotted lines in pressure and temperature graphs on the right). Regression line was fitted to all experimental points to enable calculation of relative change of unit-cell parameters for any pressure and temperature conditions. The centroids of triangles are presented as dots of matching colors.

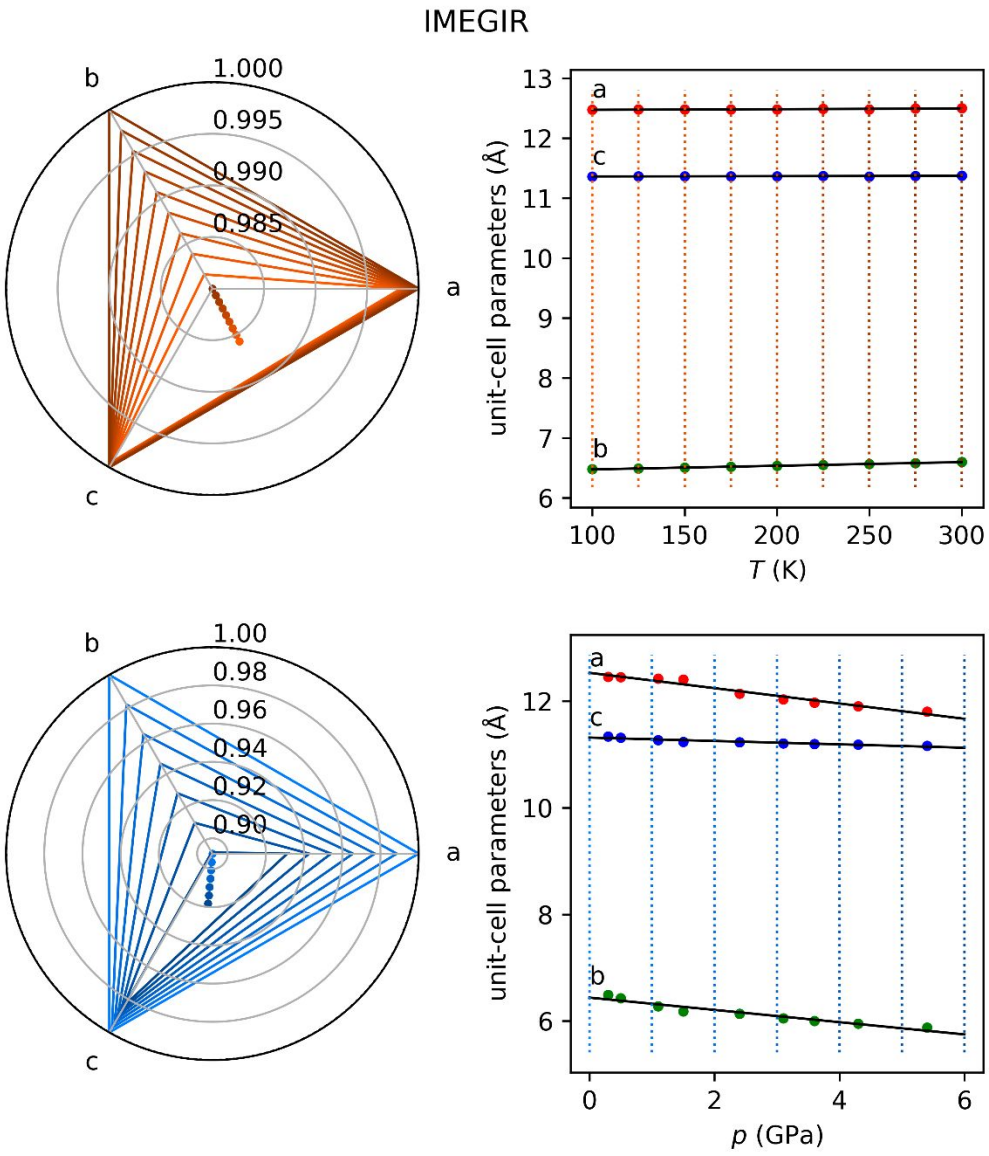

Figure S11. Change of unit-cell parameters lengths for DL-alaninium semioxalate monohydrate (refcode family:IMEGIR[13]) in temperature (100-300 K) and pressure (0.3-5.4 GPa) range (right), as well as relative changes (left) calculated for selected pressure and temperature points (marked with blue and red dotted lines in pressure and temperature graphs on the right). Regression line was fitted to all experimental points to enable calculation of relative change of unit-cell parameters for any pressure and temperature conditions. The centroids of triangles are presented as dots of matching colors.

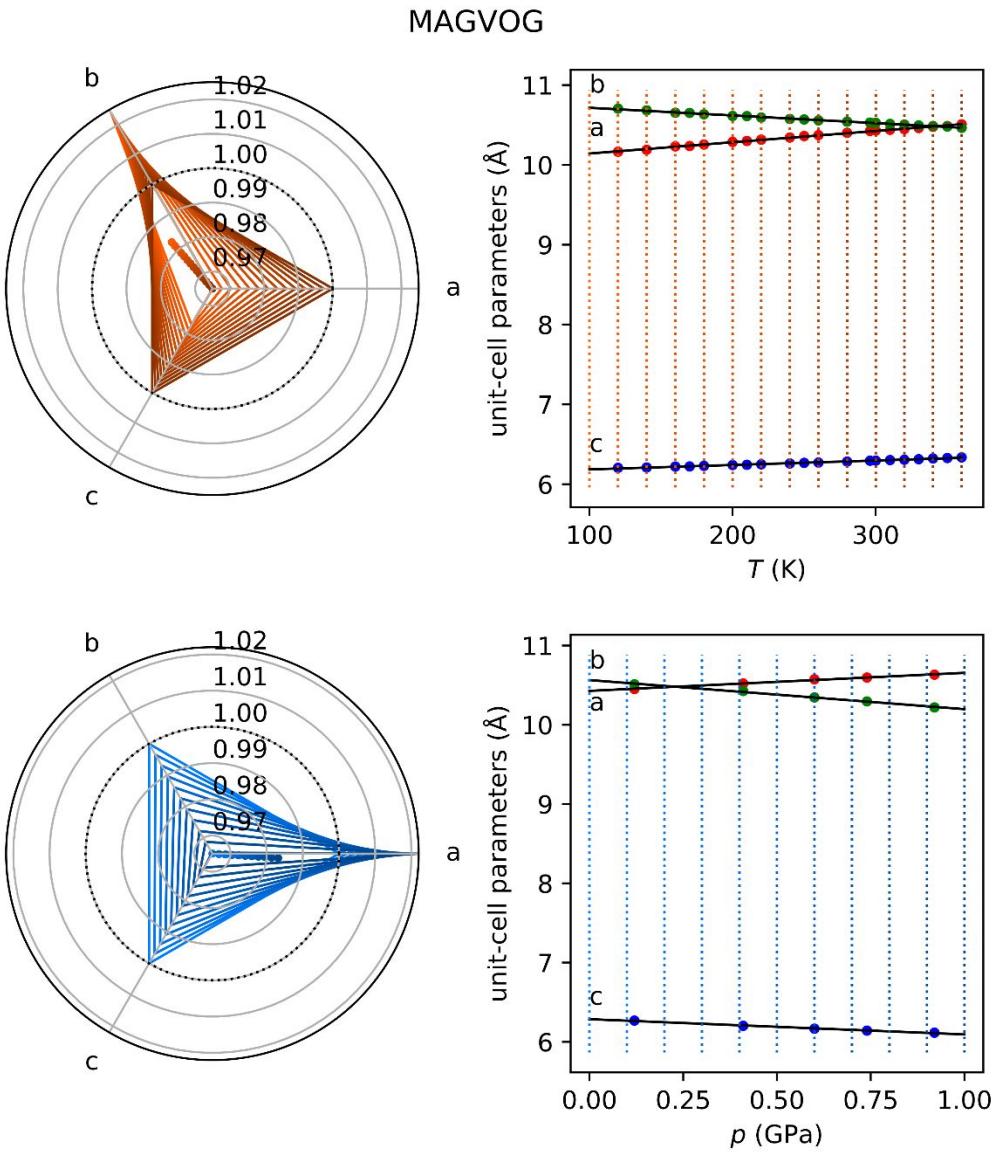

Figure S12. Change of unit-cell parameters lengths for catena-((μ_2-Ethylene-1,2-diamine-N,N')-silver(I) nitrate) polymorph I (refcode family:MAGVOG[30]) in temperature (120-360 K) and pressure (0.12-0.92 GPa) range (right), as well as relative changes (left) calculated for selected pressure and temperature points (marked with blue and red dotted lines in pressure and temperature graphs on the right). Regression line was fitted to all experimental points to enable calculation of relative change of unit-cell parameters for any pressure and temperature conditions. The centroids of triangles are presented as dots of matching colors.

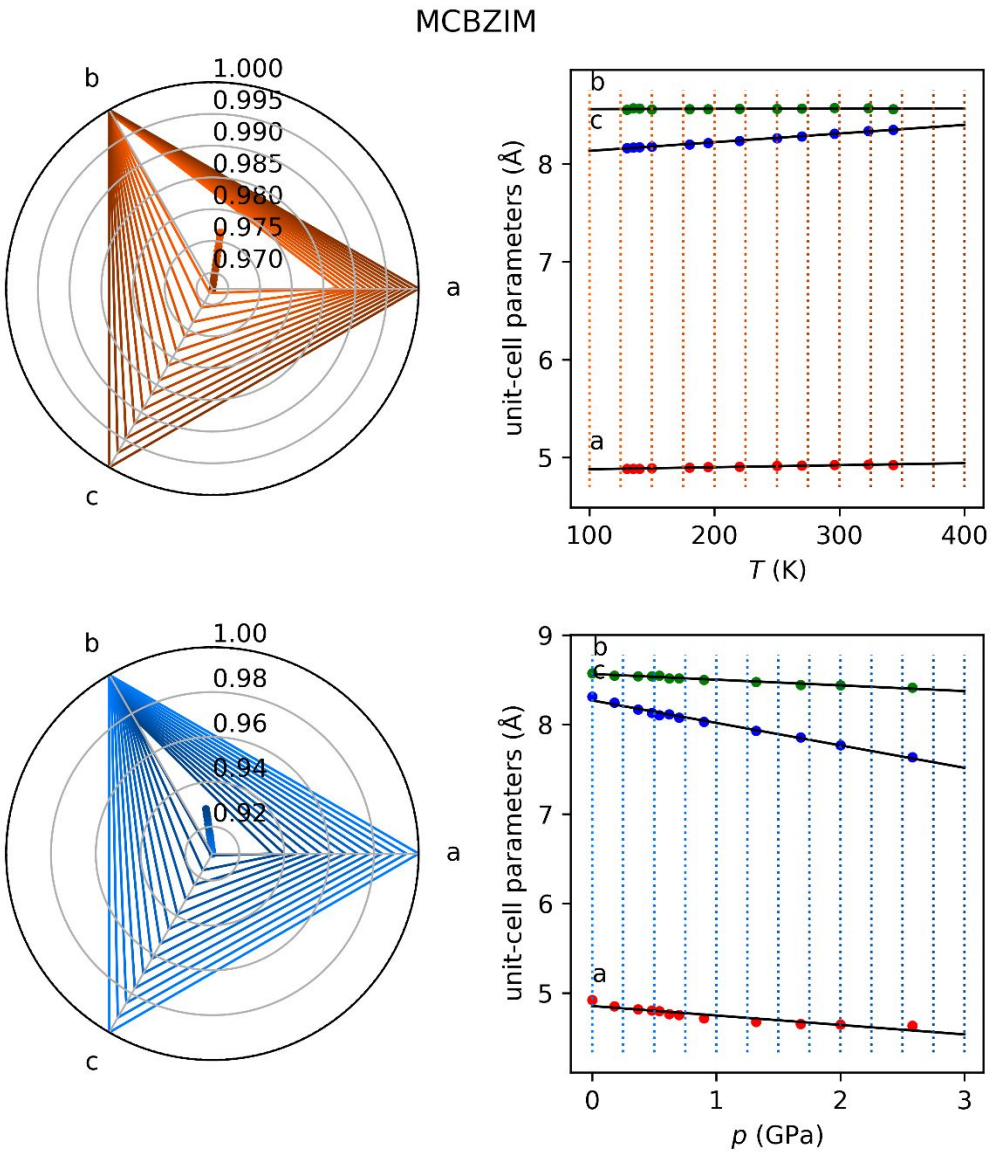

Figure S13. Change of unit-cell parameters lengths for 1,3-dihydro-2H-benzimidazole-2-thione (refcode family: MCBZIM[14]) in temperature (130-343 K) and pressure (ambient-2.58 GPa) range (right), as well as relative changes (left) calculated for selected pressure and temperature points (marked with blue and red dotted lines in pressure and temperature graphs on the right). Regression line was fitted to all experimental points to enable calculation of relative change of unit-cell parameters for any pressure and temperature conditions. The centroids of triangles are presented as dots of matching colors.

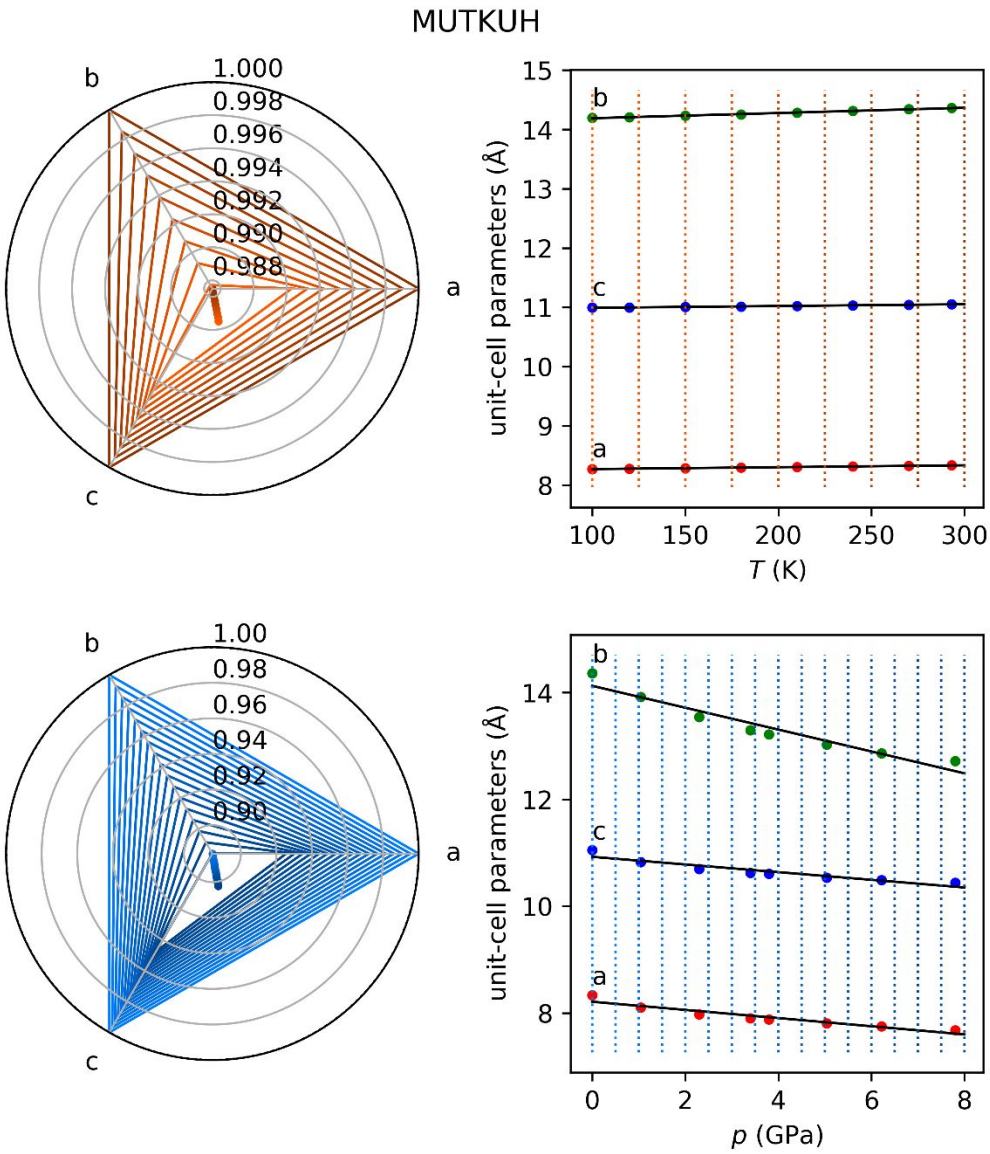

Figure S14. Change of unit-cell parameters lengths for tris(μ_2-Pyrazolato-N,N')-tri-gold(I) (refcode family:MUTKUH[15]) in temperature (100-293 K) and pressure (ambient-7.8 GPa) range (right), as well as relative changes (left) calculated for selected pressure and temperature points (marked with blue and red dotted lines in pressure and temperature graphs on the right). Regression line was fitted to all experimental points to enable calculation of relative change of unit-cell parameters for any pressure and temperature conditions. The centroids of triangles are presented as dots of matching colors.

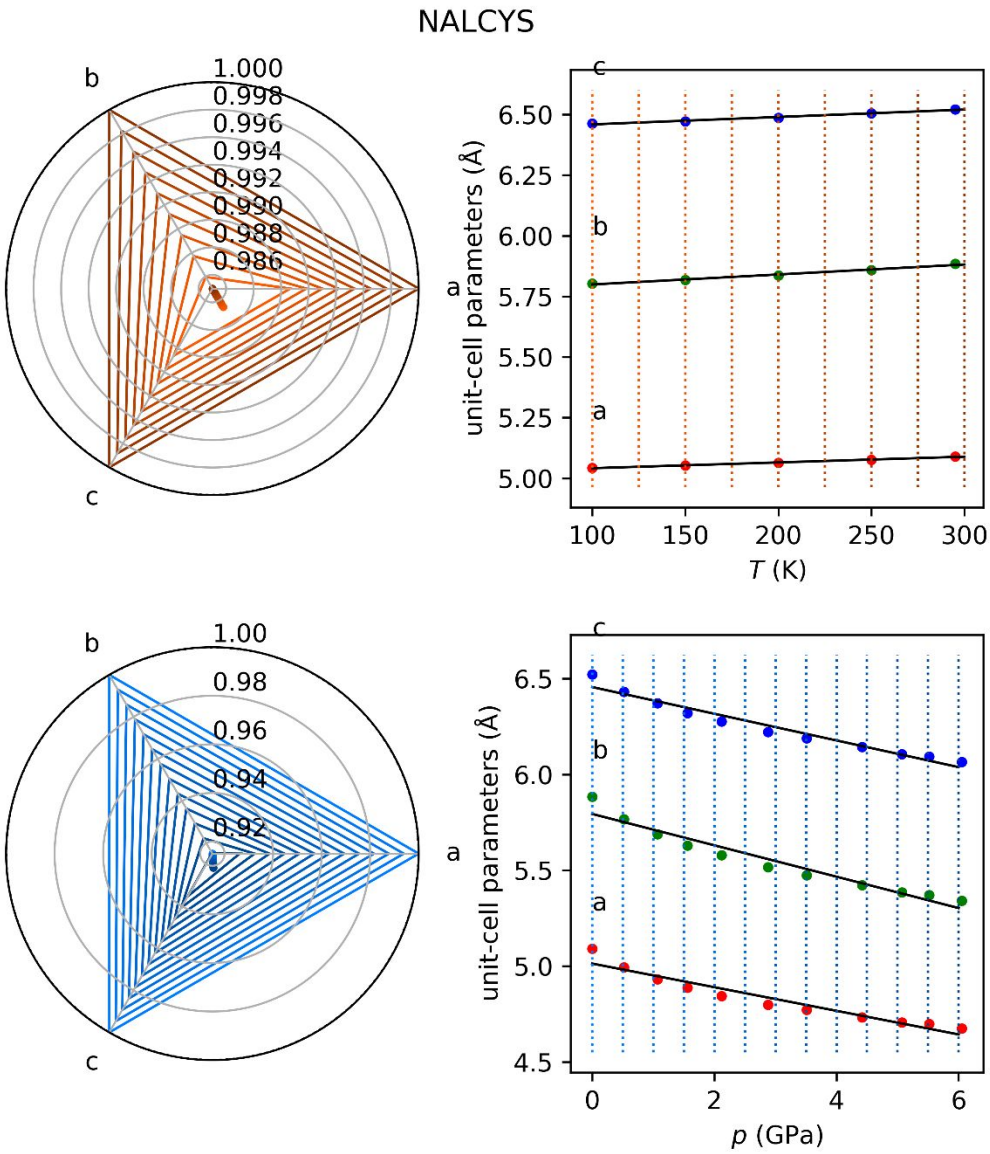

Figure S15. Change of unit-cell parameters lengths for N-acetyl-L-cysteine polymorph I (refcode family:NALCYS) in temperature (100-295 K)[16] and pressure (ambient-6.05 GPa)[17] range (right), as well as relative changes (left) calculated for selected pressure and temperature points (marked with blue and red dotted lines in pressure and temperature graphs on the right). Regression line was fitted to all experimental points to enable calculation of relative change of unit-cell parameters for any pressure and temperature conditions. The centroids of triangles are presented as dots of matching colors.

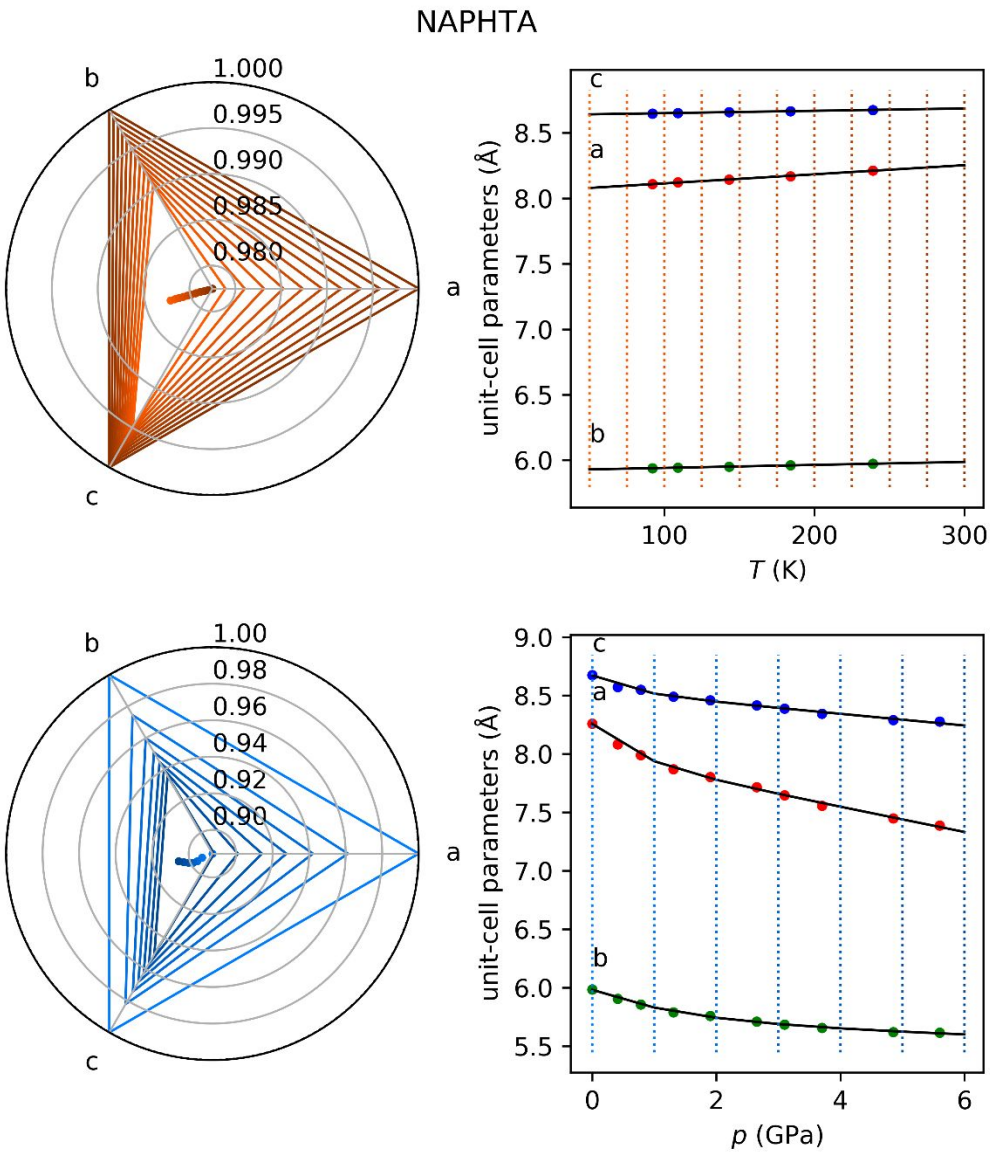

Figure S16. Change of unit-cell parameters lengths for naphthalene (refcode family:NAPHTA) in temperature (92-239 K)[18] and pressure (ambient-5.6 GPa)[19] range (right), as well as relative changes (left) calculated for selected pressure and temperature points (marked with blue and red dotted lines in pressure and temperature graphs on the right). Regression line was fitted to all experimental points to enable calculation of relative change of unit-cell parameters for any pressure and temperature conditions. The centroids of triangles are presented as dots of matching colors.

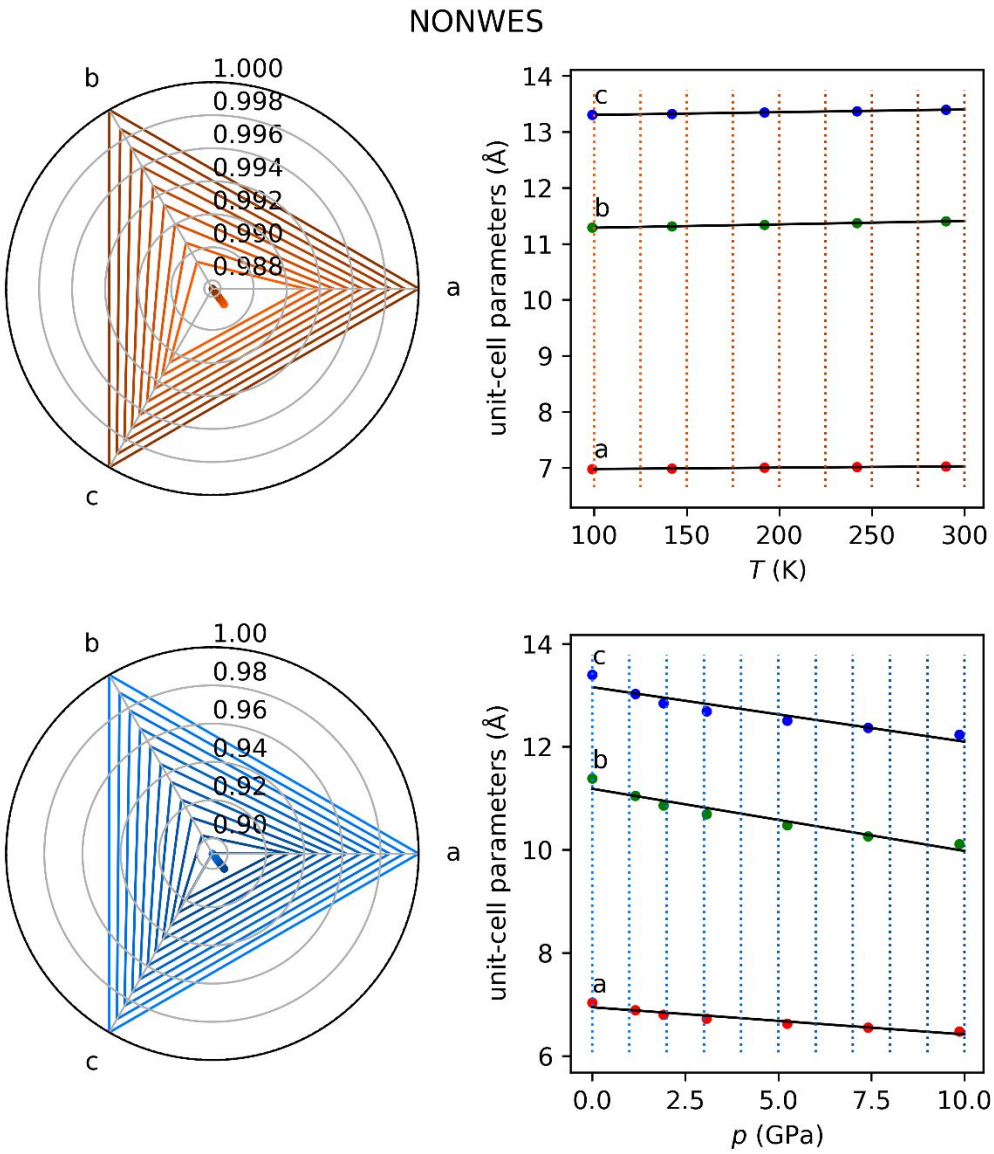

Figure S17. Change of unit-cell parameters lengths for dichloro-(1,4,7-oxadithionane)-palladium(II) polymorph *γ* (refcode family: NONWES[20]) in temperature (99-290 K) and pressure (ambient-9.86 GPa) range (right), as well as relative changes (left) calculated for selected pressure and temperature points (marked with blue and red dotted lines in pressure and temperature graphs on the right). Regression line was fitted to all experimental points to enable calculation of relative change of unit-cell parameters for any pressure and temperature conditions. The centroids of triangles are presented as dots of matching colors.

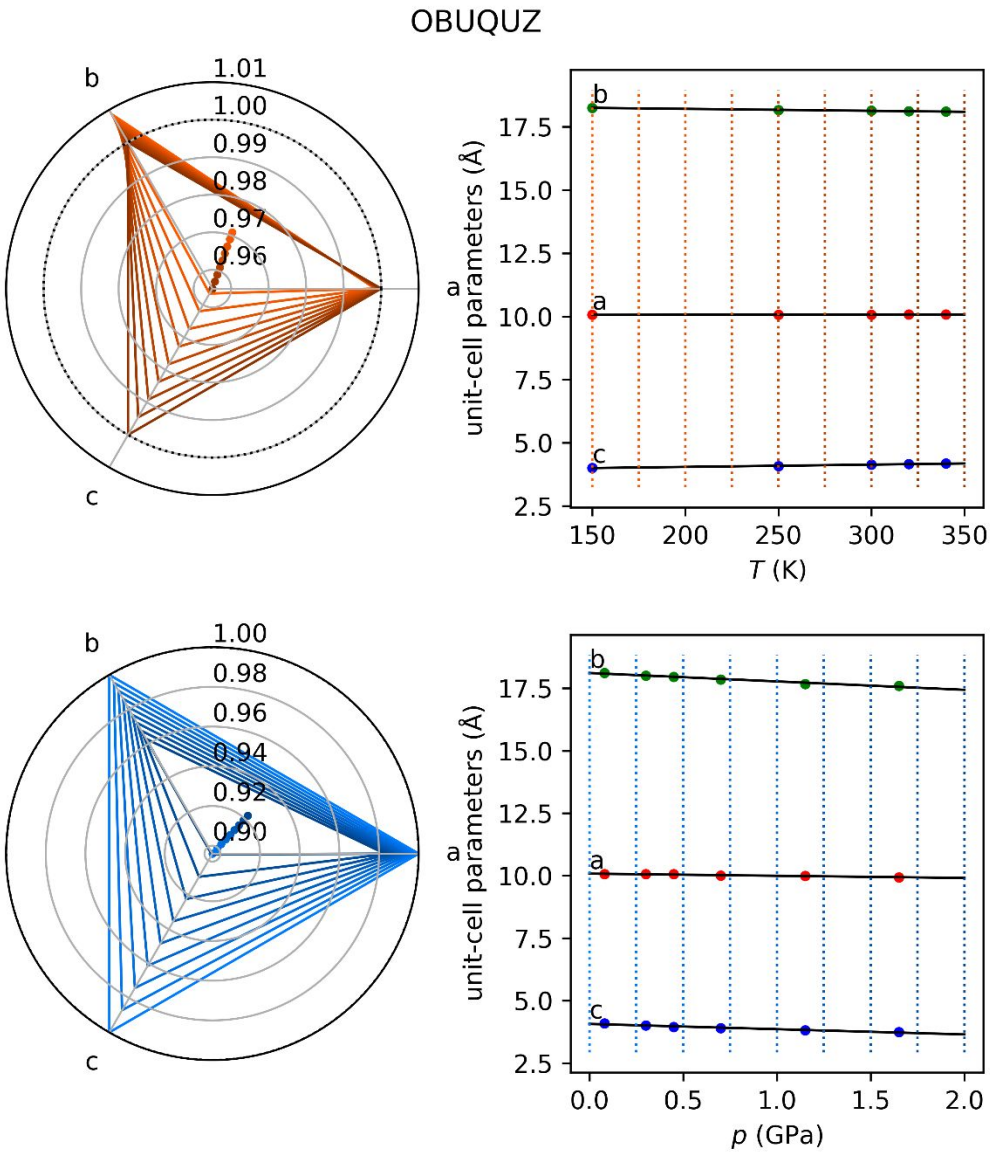

Figure S18. Change of unit-cell parameters lengths for 2-phenyl-1H-imidazole (refcode family:OBUQUZ[21]) in temperature (150-340 K) and pressure (0.08-1.65 GPa) range (right), as well as relative changes (left) calculated for selected pressure and temperature points (marked with blue and red dotted lines in pressure and temperature graphs on the right). Regression line was fitted to all experimental points to enable calculation of relative change of unit-cell parameters for any pressure and temperature conditions. The centroids of triangles are presented as dots of matching colors.

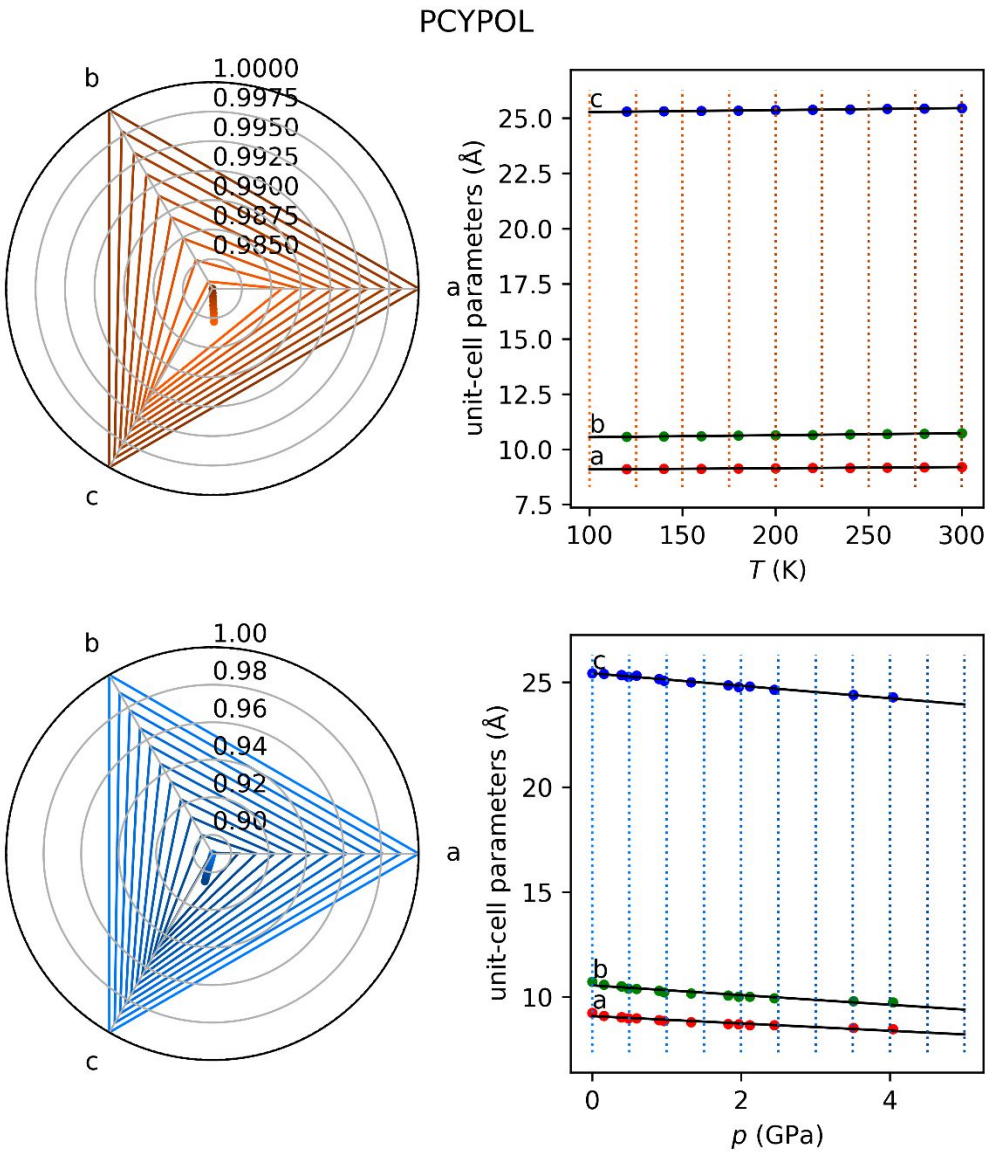

Figure S19. Change of unit-cell parameters lengths for 4-hydroxybenzonitrile *Pbcn* polymorph (refcode family: PCYPOL[22]) in temperature (120-300 K) and pressure (ambient-4.03 GPa) range (right), as well as relative changes (left) calculated for selected pressure and temperature points (marked with blue and red dotted lines in pressure and temperature graphs on the right). Regression line was fitted to all experimental points to enable calculation of relative change of unit-cell parameters for any pressure and temperature conditions. The centroids of triangles are presented as dots of matching colors.

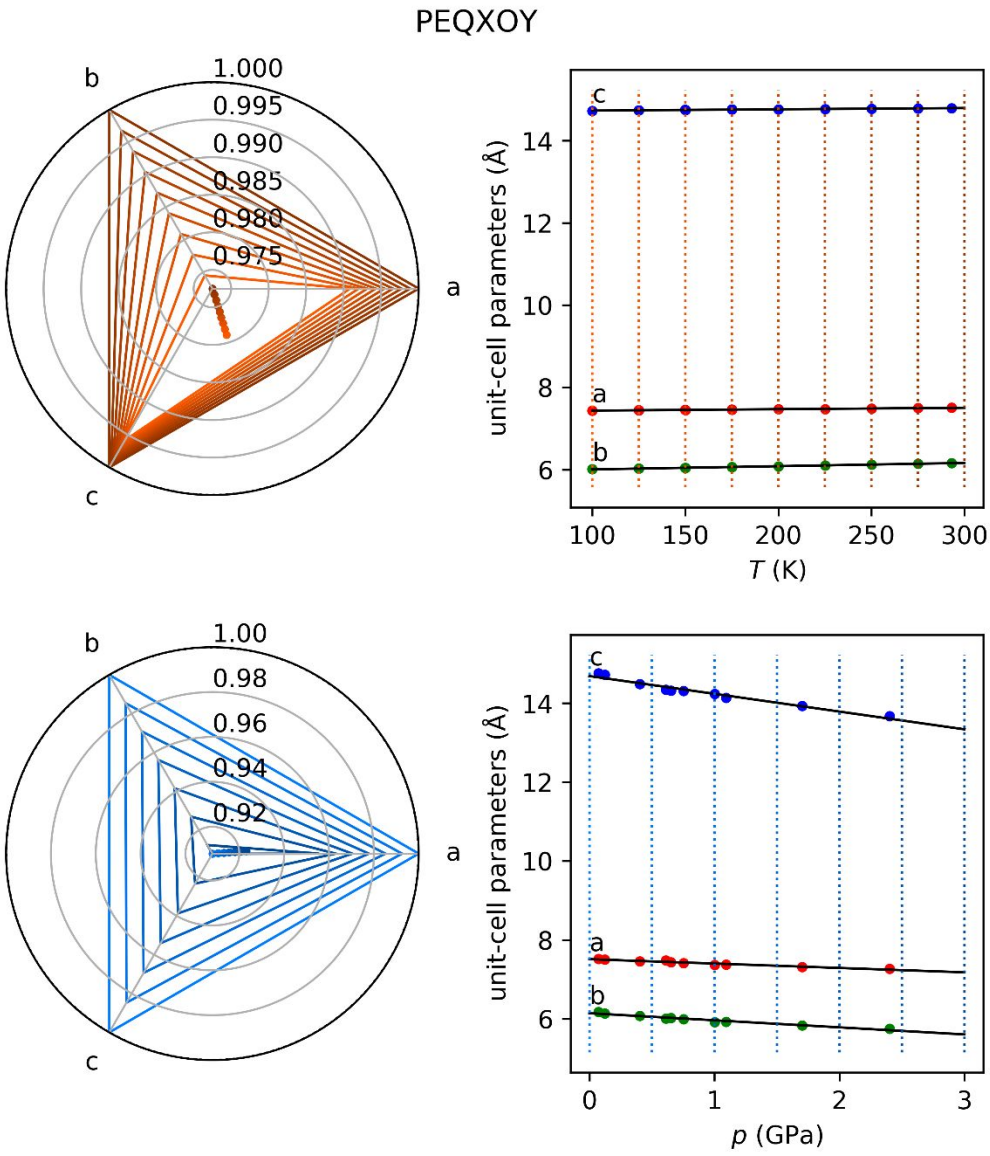

Figure S20. Change of unit-cell parameters lengths for 6-azido-1,2,3,4-tetrazolo[1,5-b]pyridazine polymorph *α* (refcode family: PEQXOY[31]) in temperature (100-293 K) and pressure (0.07-2.40 GPa) range (right), as well as relative changes (left) calculated for selected pressure and temperature points (marked with blue and red dotted lines in pressure and temperature graphs on the right). Regression line was fitted to all experimental points to enable calculation of relative change of unit-cell parameters for any pressure and temperature conditions. The centroids of triangles are presented as dots of matching colors.

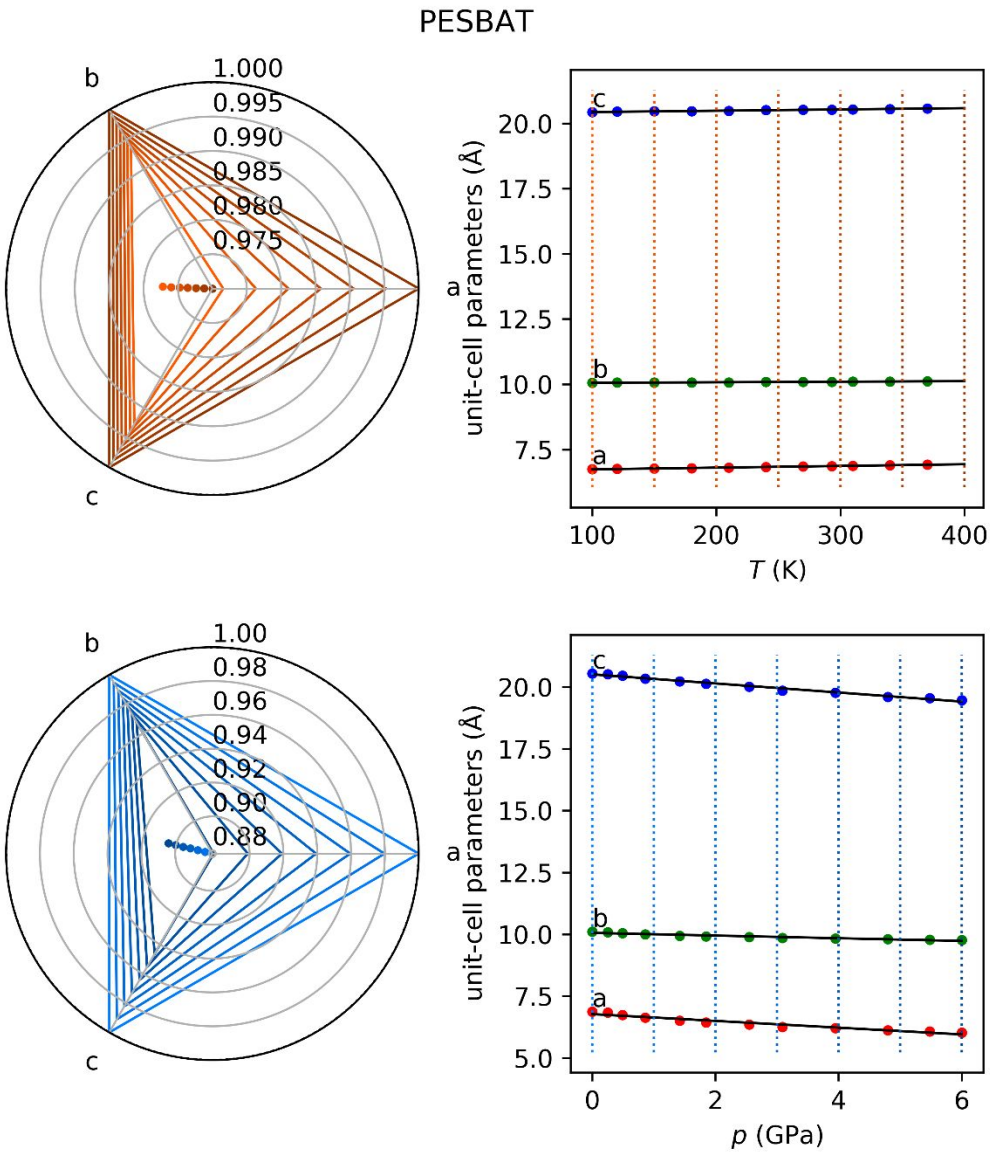

Figure S21. Change of unit-cell parameters lengths for 4-cyano-1-methylpyridin-1-ium 5,6-dichloro-2,3-dicyanosemiquinone radical anion (refcode family: PESBAT[23]) in temperature (100-370 K) and pressure (ambient-6GPa) range (right), as well as relative changes (left) calculated for selected pressure and temperature points (marked with blue and red dotted lines in pressure and temperature graphs on the right). Regression line was fitted to all experimental points to enable calculation of relative change of unit-cell parameters for any pressure and temperature conditions. The centroids of triangles are presented as dots of matching colors.

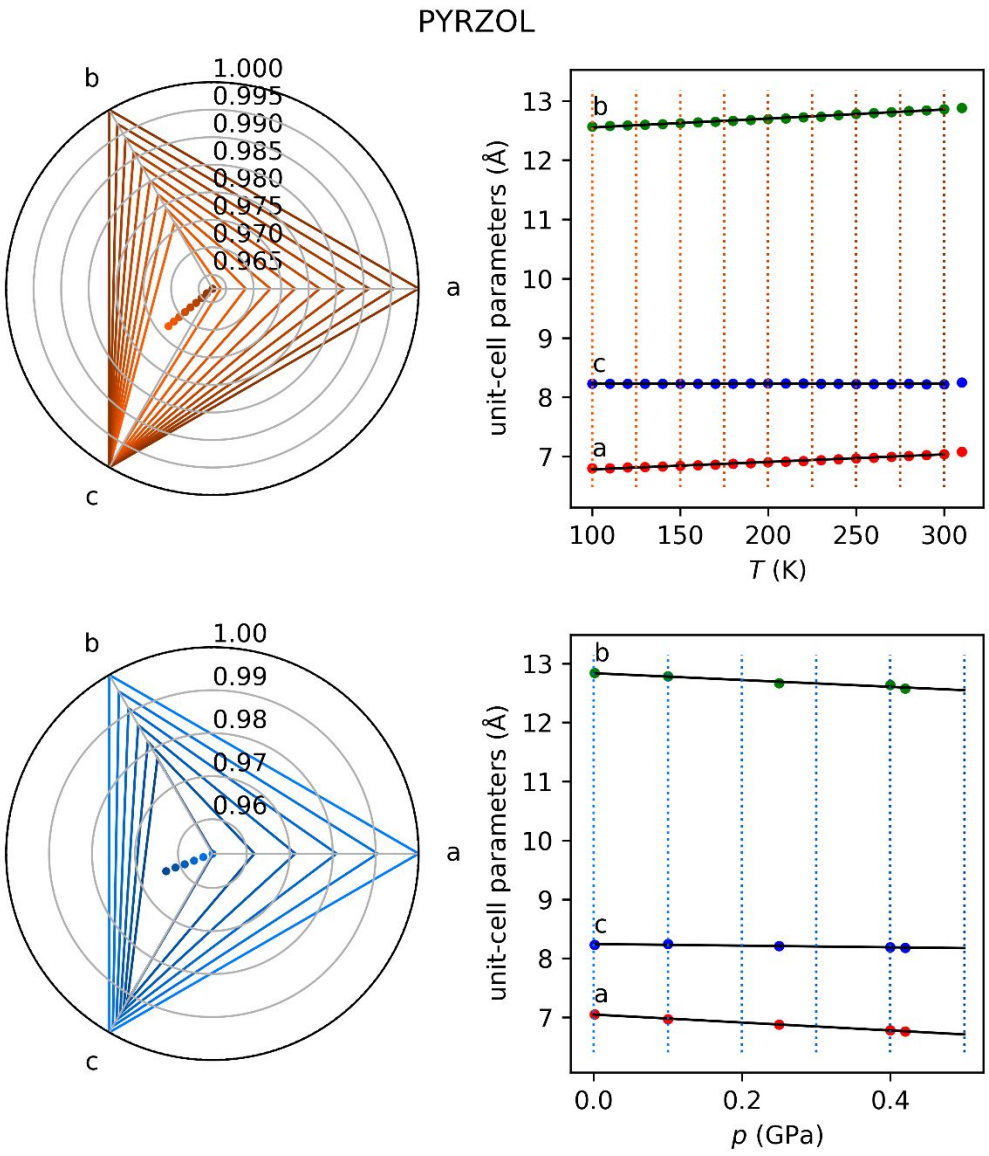

Figure S22. Change of unit-cell parameters lengths for pyrazole polymorph α (refcode family: PYRZOL[24]) in temperature (100-310 K) and pressure (ambient-0.42 GPa) range (right), as well as relative changes (left) calculated for selected pressure and temperature points (marked with blue and red dotted lines in pressure and temperature graphs on the right). Regression line was fitted to all experimental points to enable calculation of relative change of unit-cell parameters for any pressure and temperature conditions. The centroids of triangles are presented as dots of matching colors.

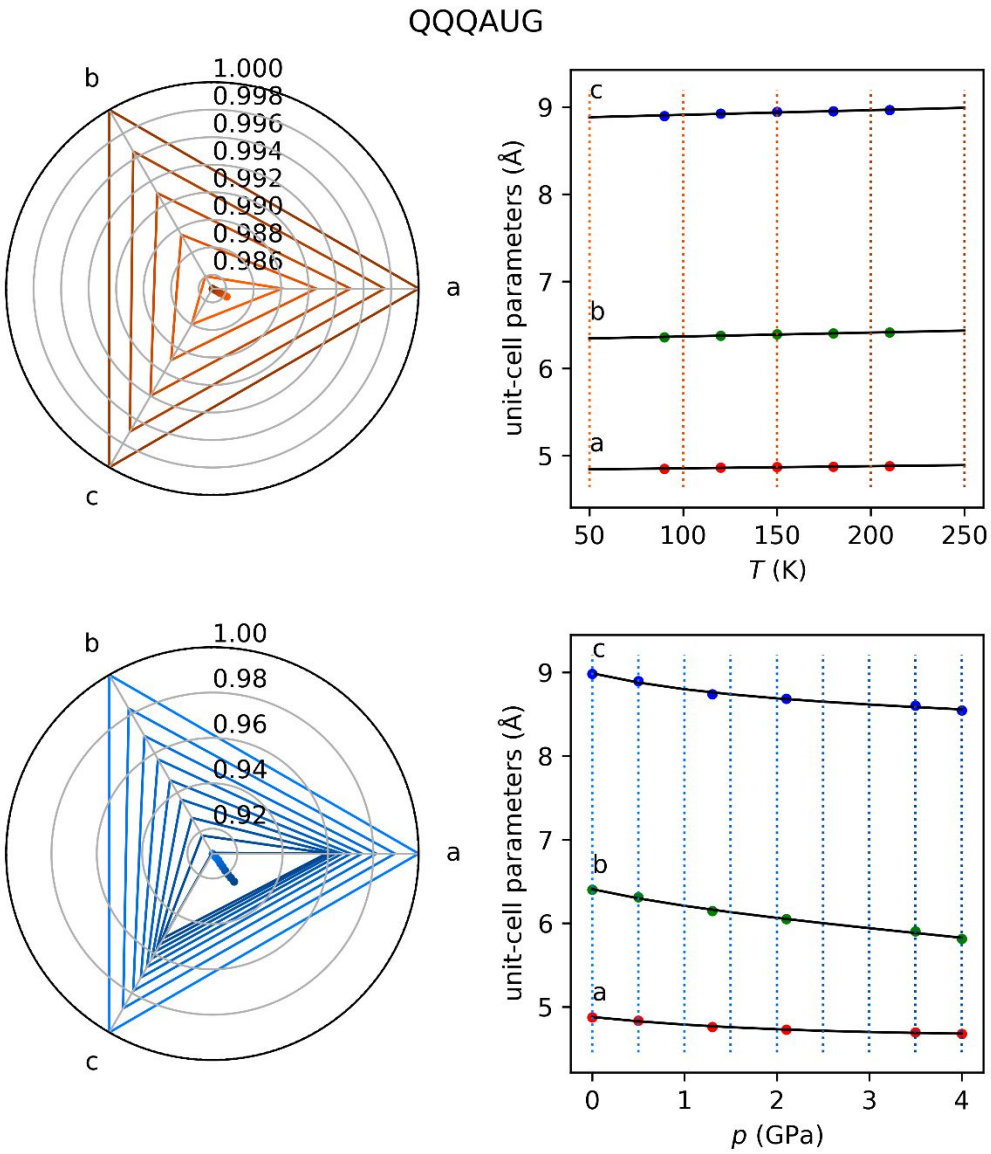

Figure S23. Change of unit-cell parameters lengths for 6-chloro-4H-1,2,4-benzothiadiazine-7-sulfonamide 1,1-dioxide polymorph I (refcode family:QQQAUG) in temperature (90-210 K)[25] and pressure (0.5-4.0 GPa)[26] range (right), as well as relative changes (left) calculated for selected pressure and temperature points (marked with blue and red dotted lines in pressure and temperature graphs on the right). Regression line was fitted to all experimental points to enable calculation of relative change of unit-cell parameters for any pressure and temperature conditions. The centroids of triangles are presented as dots of matching colors.

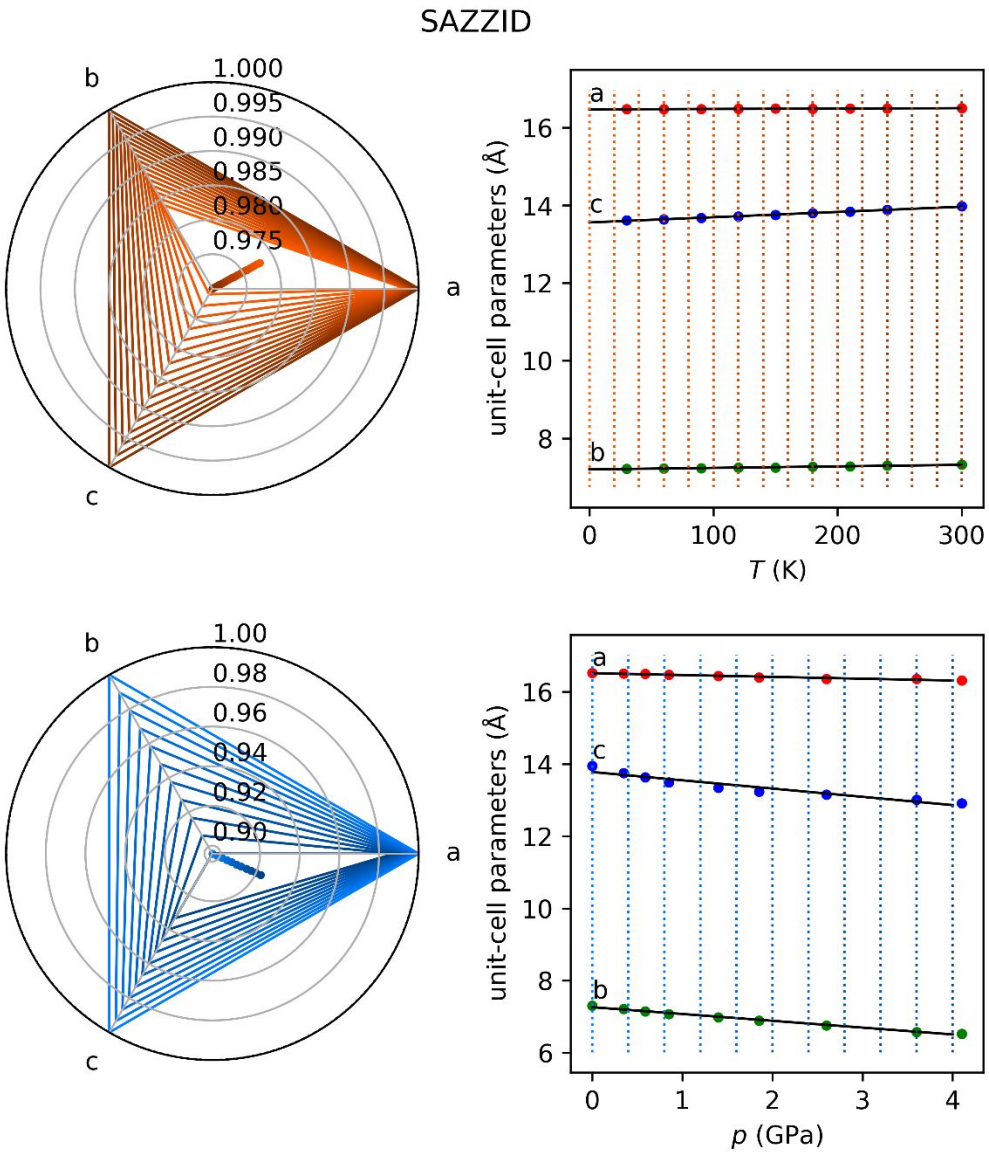

Figure S24. Change of unit-cell parameters lengths for bis(4-chloropyridinium) tetrachloro-cobalt(II) (refcode family:SAZZID[32]) in temperature (30-300 K) and pressure (ambient-4.10 GPa) range (right), as well as relative changes (left) calculated for selected pressure and temperature points (marked with blue and red dotted lines in pressure and temperature graphs on the right). Regression line was fitted to all experimental points to enable calculation of relative change of unit-cell parameters for any pressure and temperature conditions. The centroids of triangles are presented as dots of matching colors.

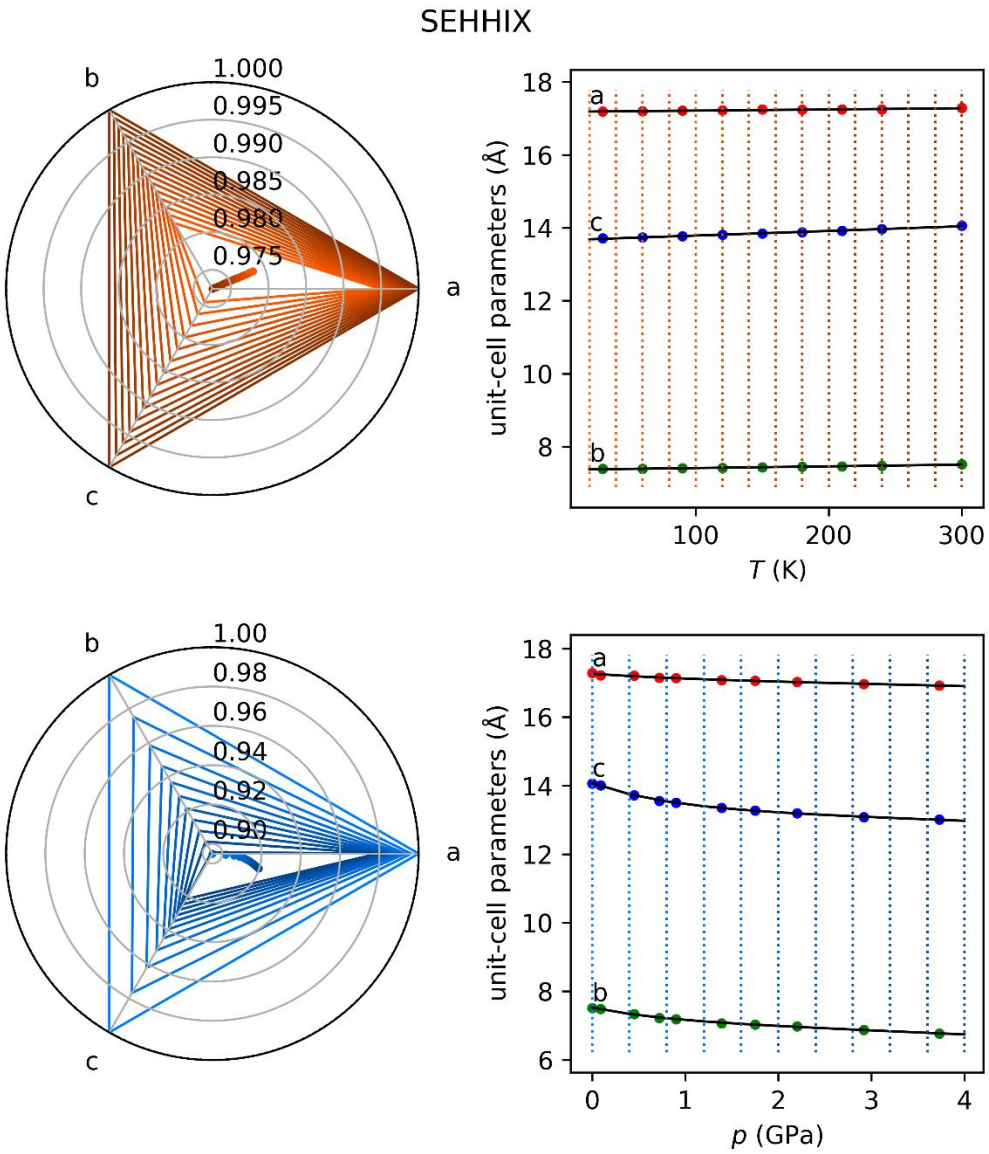

Figure S25. Change of unit-cell parameters lengths for bis(4-chloropyridinium) tetrabromo-cobalt(II) (refcode family: SEHHIX[32]) in temperature (30-300 K) and pressure (ambient-3.73 GPa) range (right), as well as relative changes (left) calculated for selected pressure and temperature points (marked with blue and red dotted lines in pressure and temperature graphs on the right). Regression line was fitted to all experimental points to enable calculation of relative change of unit-cell parameters for any pressure and temperature conditions. The centroids of triangles are presented as dots of matching colors.

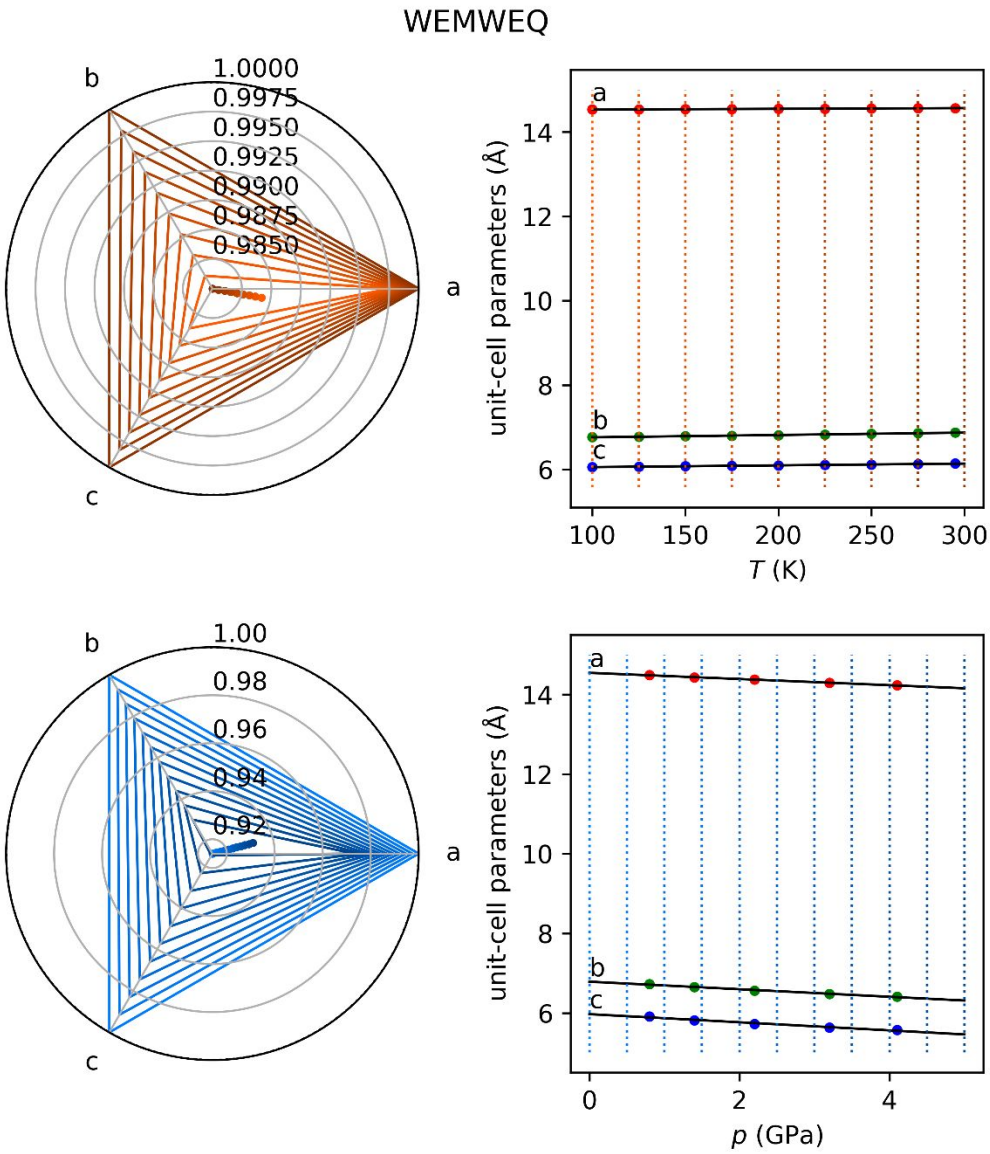

Figure S26. Change of unit-cell parameters lengths for 2-(trimethylamino)acetic acid (betaine; refcode family: WEMWEQ) in temperature (100-295 K)[27] and pressure (0.80-4.10 GPa)[28] range (right), as well as relative changes (left) calculated for selected pressure and temperature points (marked with blue and red dotted lines in pressure and temperature graphs on the right). Regression line was fitted to all experimental points to enable calculation of relative change of unit-cell parameters for any pressure and temperature conditions. The centroids of triangles are presented as dots of matching colors.

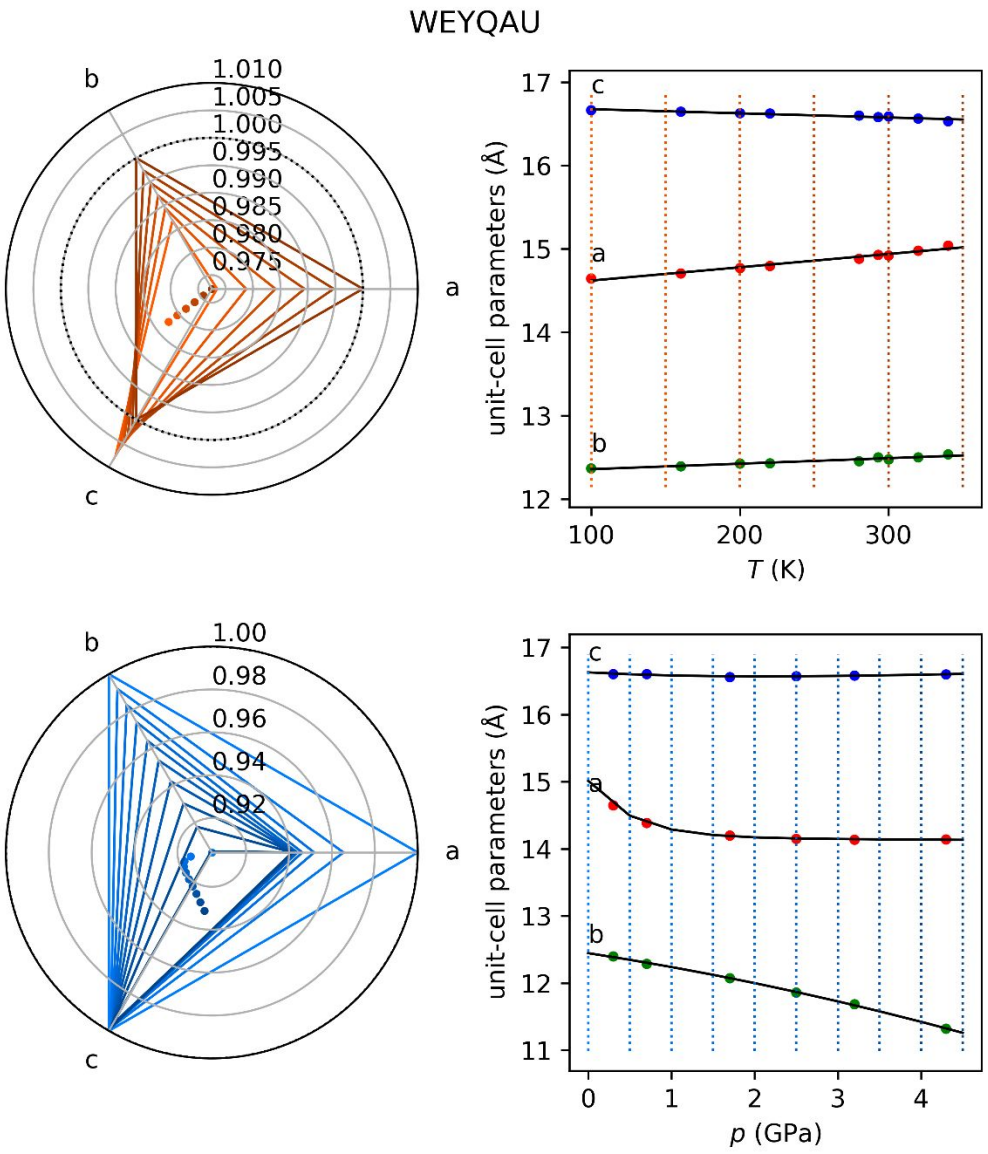

Figure S27. Change of unit-cell parameters lengths for catena-(1-Ethyl-3-methylimidazol-3-ium (μ_4-benzene-1,3,5-tricarboxylato)-manganese) (refcode family: WEYQAU) in temperature (100-340 K)[33] and pressure (0.3-4.3 GPa)[34] range (right), as well as relative changes (left) calculated for selected pressure and temperature points (marked with blue and red dotted lines in pressure and temperature graphs on the right). Regression line was fitted to all experimental points to enable calculation of relative change of unit-cell parameters for any pressure and temperature conditions. The centroids of triangles are presented as dots of matching colors.

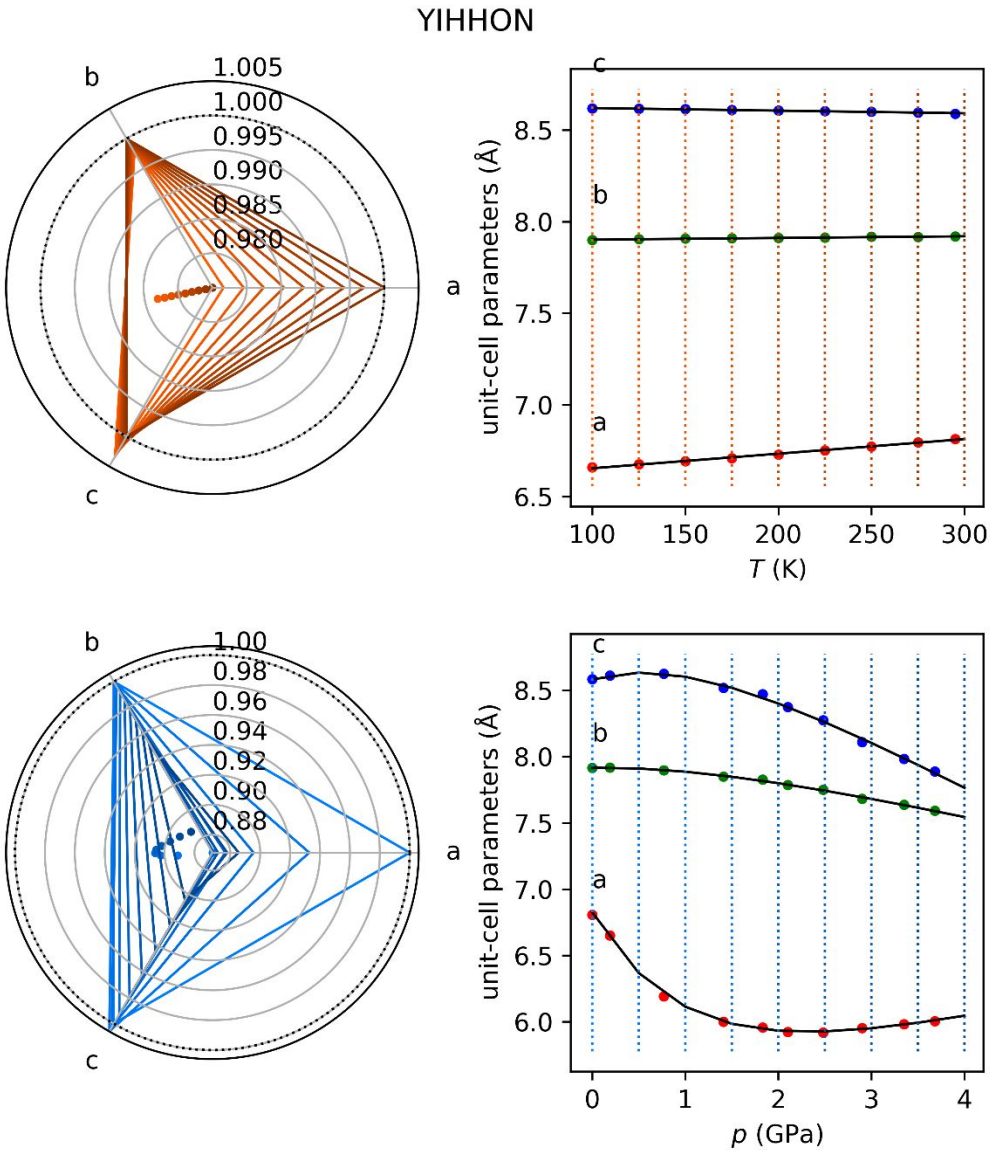

Figure S28. Change of unit-cell parameters lengths for N-Trideuteromethylammonioacetate (refcode family: YIHHON) in temperature (100-295 K)[27] and pressure (ambient-3.68 GPa)[28] range (right), as well as relative changes (left) calculated for selected pressure and temperature points (marked with blue and red dotted lines in pressure and temperature graphs on the right). Regression line was fitted to all experimental points to enable calculation of relative change of unit-cell parameters for any pressure and temperature conditions. The centroids of triangles are presented as dots of matching colors.

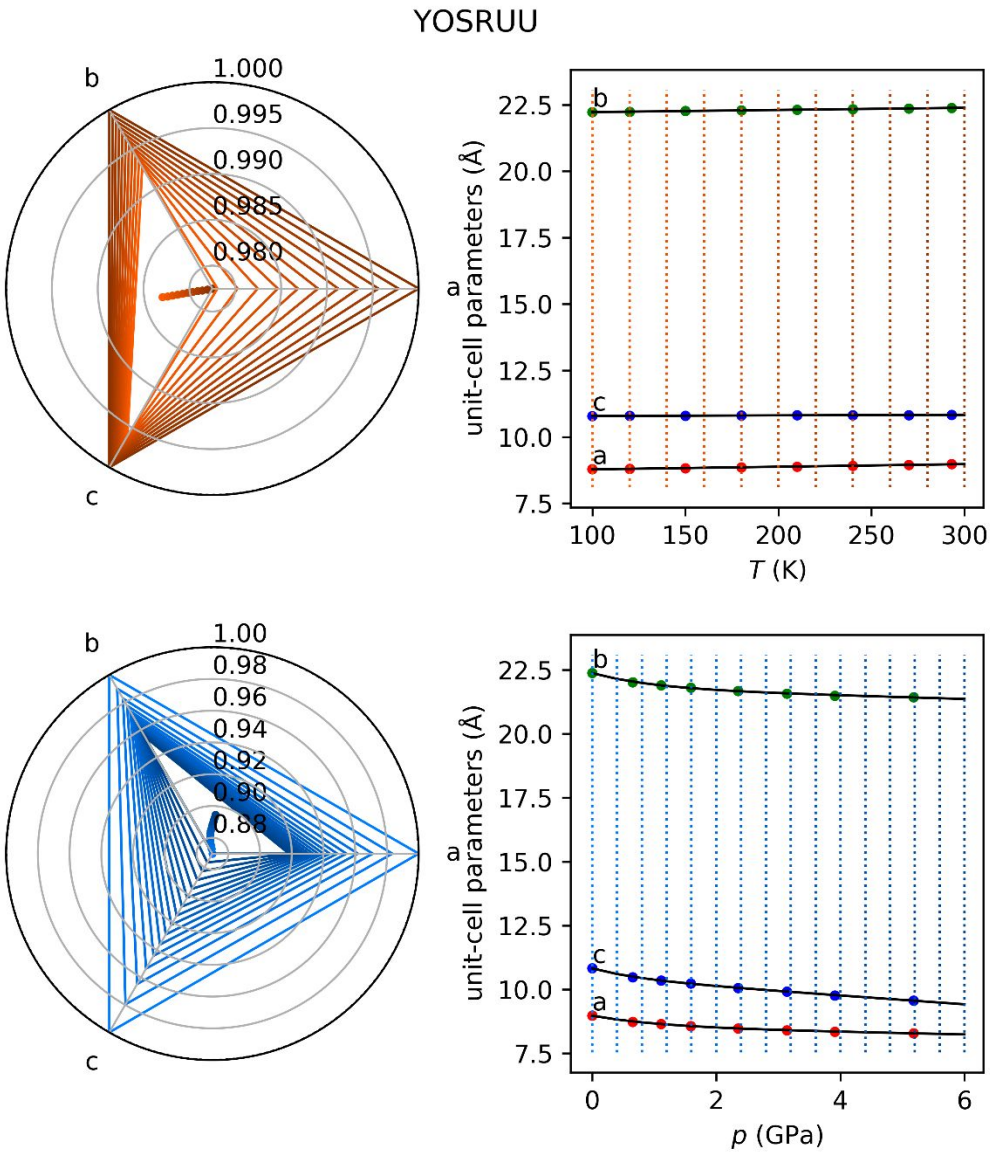

Figure S29. Change of unit-cell parameters lengths for tris(μ_2-3,4,5-Trimethylpyrazolato-N,N')-tri-gold(i) (refcode family: YOSRUU[15]) in temperature (100-293 K) and pressure (ambient-5.18 GPa) range (right), as well as relative changes (left) calculated for selected pressure and temperature points (marked with blue and red dotted lines in pressure and temperature graphs on the right). Regression line was fitted to all experimental points to enable calculation of relative change of unit-cell parameters for any pressure and temperature conditions. The centroids of triangles are presented as dots of matching colors.

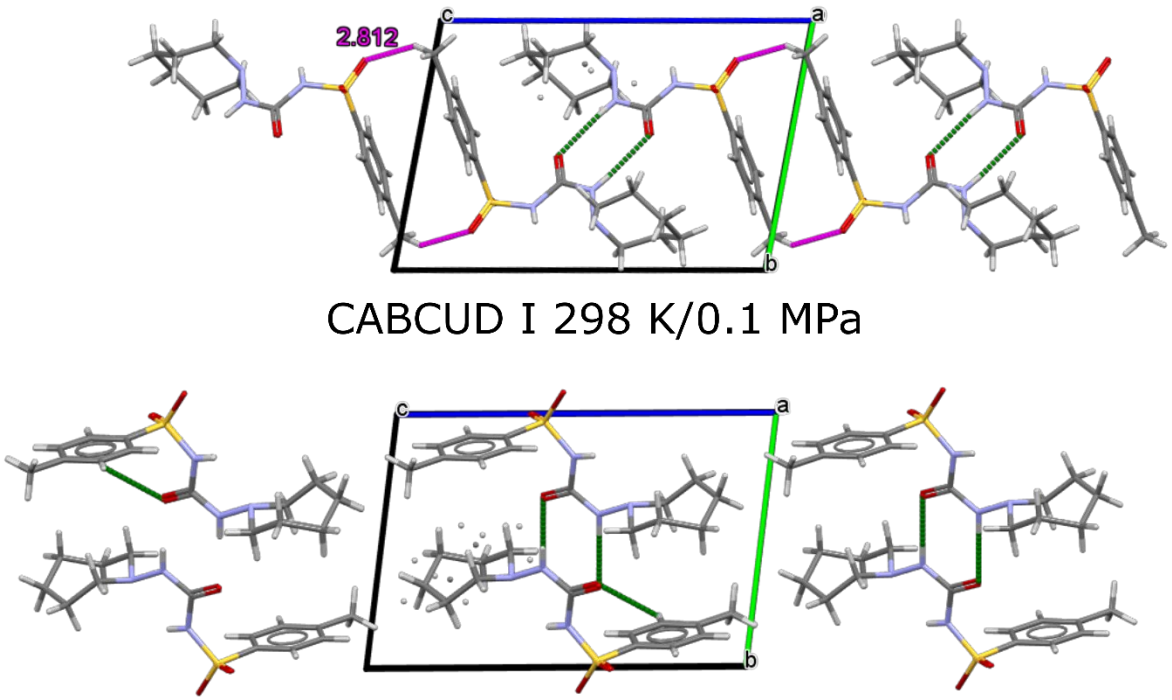

Figure S30 Crystal packing in CABCUD polymorph I (top, refcode: CABCUD26[7]) and II (bottom, refcode: CABCUD35[7]) shown along direction [100]. Hydrogen bonds are marked in green, while longer contacts considered to be too long to be recognized as hydrogen bonds are marked in magenta.

S4. References

(1) Macrae, C. F.; Bruno, I. J.; Chisholm, J. A.; Edgington, P. R.; McCabe, P.; Pidcock, E.; Rodriguez-Monge, L.; Taylor, R.; van de Streek, J.; Wood, P. A. *Mercury CSD 2.0* – New Features for the Visualization and Investigation of Crystal Structures. *J. Appl. Crystallogr.* **2008**, *41* (2), 466–470. https://doi.org/10.1107/S0021889807067908.

(2) Casati, N.; Kleppe, A.; Jephcoat, A. P.; Macchi, P. Putting Pressure on Aromaticity along with in Situ Experimental Electron Density of a Molecular Crystal. *Nat. Commun.* **2016**, *7* (1), 1–8. https://doi.org/10.1038/ncomms10901.

(3) Paliwoda, D.; Szafrański, M.; Hanfland, M.; Katrusiak, A. A Giant 2-Dimensional Dielectric Response in a Compressed Hydrogen-Bonded Hybrid Organic–Inorganic Salt. *J. Mater. Chem. C* **2018**, *6* (28), 7689–7699. https://doi.org/10.1039/C8TC02464B.

(4) Szafrański, M. Simple Guanidinium Salts Revisited: Room–Temperature Ferroelectricity in Hydrogen-Bonded Supramolecular Structures. *J. Phys. Chem. B* **2011**, *115* (27), 8755–8762. https://doi.org/10.1021/jp202192k.

(5) Szafrański, M. Effect of High Pressure on the Supramolecular Structures of Guanidinium Based Ferroelectrics. *CrystEngComm* **2014**, *16* (27), 6250–6256. https://doi.org/10.1039/C4CE00697F.

(6) Fedorov, A. Y.; Rychkov, D. A.; Losev, E. A.; Zakharov, B. A.; Stare, J.; Boldyreva, E. V. Effect of Pressure on Two Polymorphs of Tolazamide: Why No Interconversion? *CrystEngComm* **2017**, *19* (16), 2243–2252. https://doi.org/10.1039/C6CE02527G.
(7) Fedorov, A. Y.; Rychkov, D. A.; Losev, E. A.; Drebushchak, T. N.; Boldyreva, E. V. Completing the Picture of Tolaza-mide Polymorphism under Extreme Conditions: A Low-Temperature Study. *Acta Crystallogr., Sect. C: Struct. Chem.* **2019**, *75* (5), 598–608. https://doi.org/10.1107/S2053229619005217.
(8) Ogborn, J. M.; Collings, I. E.; Moggach, S. A.; Thompson, A. L.; Goodwin, A. L. Supramolecular Mechanics in a Metal–Organic Framework. *Chem. Sci.* **2012**, *3* (10), 3011–3017. https://doi.org/10.1039/C2SC20596C.
(9) Roszak, K.; Katrusiak, A.; Katrusiak, A. High-Pressure Preference for the Low *Z*′ Polymorph of a Molecular Crystal. *Cryst. Growth Des.* **2016**, *16* (7), 3947–3953. https://doi.org/10.1021/acs.cgd.6b00521.
(10) Naumov, P.; Ishizawa, N.; Wang, J.; Pejov, L.; Pumera, M.; Lee, S. C. On the Origin of the Solid-State Thermochromism and Thermal Fatigue of Polycyclic Overcrowded Enes. *J. Phys. Chem. A* **2011**, *115* (30), 8563–8570. https://doi.org/10.1021/jp2040339.
(11) Johnstone, R. D. L.; Allan, D.; Lennie, A.; Pidcock, E.; Valiente, R.; Rodríguez, F.; Gonzalez, J.; Warren, J.; Parsons, S. The Effect of Pressure on the Crystal Structure of Bianthrone. *Acta Crystallogr., Sect. B: Struct. Sci.* **2011**, *67* (3), 226–237. https://doi.org/10.1107/S0108768111009657.
(12) Ostrowska, K.; Kropidłowska, M.; Katrusiak, A. High-Pressure Crystallization and Structural Transformations in Compressed R,S-Ibuprofen. *Cryst. Growth Des.* **2015**, *15* (3), 1512–1517. https://doi.org/10.1021/cg5018888.
(13) Zakharov, B. A.; Boldyreva, E. V. DL-Alaninium Semi-Oxalate Monohydrate. *Acta Crystallogr., Sect. C: Cryst. Struct. Commun.* **2011**, *67* (2), o47–o51. https://doi.org/10.1107/S0108270110053655.
(14) Tomkowiak, H.; Katrusiak, A. High Pressure Effects on Zwitterionic and Thione Mesomeric Contributions in 2-Benzimidazole-2-Thione. *J. Phys. Chem. C* **2017**, *121* (34), 18830–18836. https://doi.org/10.1021/acs.jpcc.7b06083.
(15) Woodall, C. H.; Fuertes, S.; Beavers, C. M.; Hatcher, L. E.; Parlett, A.; Shepherd, H. J.; Christensen, J.; Teat, S. J.; Intissar, M.; Rodrigue-Witchel, A.; Suffren, Y.; Reber, C.; Hendon, C. H.; Tiana, D.; Walsh, A.; Raithby, P. R. Tunable Trimers: Using Temperature and Pressure to Control Luminescent Emission in Gold(I) Pyrazolate-Based Trimers. *Chem. Eur. J.* **2014**, *20* (51), 16933–16942. https://doi.org/10.1002/chem.201404058.
(16) Minkov, V. S.; Boldyreva, E. V.; Drebushchak, T. N.; Görbitz, C. H. Stabilizing Structures of Cysteine-Containing Crystals with Respect to Variations of Temperature and Pressure by Immobilizing Amino Acid Side Chains. *CrystEngComm* **2012**, *14* (18), 5943–5954. https://doi.org/10.1039/C2CE25241D.
(17) Minkov, V. S.; Boldyreva, E. V. Weak Hydrogen Bonds Formed by Thiol Groups in N-Acetyl-L-Cysteine and Their Response to the Crystal Structure Distortion on Increasing Pressure. *J. Phys. Chem. B* **2013**, *117* (46), 14247–14260. https://doi.org/10.1021/jp4068872.
(18) Brock, C. P.; Dunitz, J. D. Temperature Dependence of Thermal Motion in Crystalline Naphthalene. *Acta Crystallogr., Sect. B: Struct. Crystallogr. Cryst. Chem.* **1982**, *38* (8), 2218–2228. https://doi.org/10.1107/S0567740882008358.

(19) Likhacheva, A. Y.; Rashchenko, S. V.; Litasov, K. D. High-Pressure Structural Properties of Naphthalene up to 6 GPa. *J. Appl. Crystallogr.* **2014**, *47* (3), 984–991. https://doi.org/10.1107/S1600576714005937.
(20) Tidey, J. P.; Wong, H. L. S.; McMaster, J.; Schröder, M.; Blake, A. J. High-Pressure Studies of Three Polymorphs of a Palladium(II) Oxathioether Macrocyclic Complex. *Acta Crystallogr., Sect. B: Struct. Sci., Cryst. Eng. Mater.* **2016**, *72* (3), 357–371. https://doi.org/10.1107/S2052520616007435.
(21) Sikora, M.; Bernatowicz, P.; Szafrański, M.; Katrusiak, A. Quasistatic Disorder of NH···N Bonds and Elastic-Properties Relationship in 2-Phenylimidazole Crystals. *J. Phys. Chem. C* **2014**, *118* (13), 7049–7056. https://doi.org/10.1021/jp501187v.
(22) Collings, I. E.; Hanfland, M. Packing Rearrangements in 4-Hydroxycyanobenzene Under Pressure. *Molecules* **2019**, *24* (9), 1759. https://doi.org/10.3390/molecules24091759.
(23) Bogdanov, N. E.; Milašinović, V.; Zakharov, B. A.; Boldyreva, E. V.; Molčanov, K. Pancake-Bonding of Semi-quinone Radicals under Variable Temperature and Pressure Conditions. *Acta Crystallogr., Sect. B: Struct. Sci., Cryst. Eng. Mater.* **2020**, *76* (2), 285–291. https://doi.org/10.1107/S2052520620002772.
(24) Sikora, M.; Katrusiak, A. Pressure-Controlled Neutral–Ionic Transition and Disordering of NH···N Hydrogen Bonds in Pyrazole. *J. Phys. Chem. C* **2013**, *117* (20), 10661–10668. https://doi.org/10.1021/jp401389v.
(25) Fernandes, P.; Shankland, K.; David, W. I. F.; Markvardsen, A. J.; Florence, A. J.; Shankland, N.; Leech, C. K. A Differential Thermal Expansion Approach to Crystal Structure Determination from Powder Diffraction Data. *J. Appl. Crystallogr.* **2008**, *41* (6), 1089–1094. https://doi.org/10.1107/S0021889808030872.
(26) Oswald, I. D. H.; Lennie, A. R.; Pulham, C. R.; Shankland, K. High-Pressure Structural Studies of the Pharmaceutical, Chlorothiazide. *CrystEngComm* **2010**, *12* (9), 2533–2540. https://doi.org/10.1039/C001355B.
(27) Kapustin, E. A.; Minkov, V. S.; Boldyreva, E. V. Sarcosine and Betaine Crystals upon Cooling: Structural Motifs Unstable at High Pressure Become Stable at Low Temperatures. *Phys. Chem. Chem. Phys.* **2015**, *17* (5), 3534–3543. https://doi.org/10.1039/C4CP05094K.
(28) Kapustin, E. A.; Minkov, V. S.; Boldyreva, E. V. Effect of Pressure on Methylated Glycine Derivatives: Relative Roles of Hydrogen Bonds and Steric Repulsion of Methyl Groups. *Acta Crystallogr., Sect. B: Struct. Sci., Cryst. Eng. Mater.* **2014**, *70* (3), 517–532. https://doi.org/10.1107/S205252061401035X.
(29) Ovcharenko, V.; Romanenko, G.; Polushkin, A.; Letyagin, G.; Bogomyakov, A.; Fedin, M.; Maryunina, K.; Nishihara, S.; Inoue, K.; Petrova, M.; Morozov, V.; Zueva, E. Pressure-Controlled Migration of Paramagnetic Centers in a Heterospin Crystal. *Inorg. Chem.* **2019**, *58* (14), 9187–9194. https://doi.org/10.1021/acs.inorgchem.9b00815.
(30) Cai, W.; Katrusiak, A. Giant Negative Linear Compression Positively Coupled to Massive Thermal Expansion in a Metal–Organic Framework. *Nat. Commun.* **2014**, *5* (1), 1–8. https://doi.org/10.1038/ncomms5337.
(31) Olejniczak, A.; Katrusiak, A.; Podsiadło, M.; Katrusiak, A. Short N···N and CH···N Contacts in the Ambient and High-Pressure Polymorphs of a High-Nitrogen-Content Compound. *Cryst. Growth Des.* **2019**, *19* (3), 1832–1838. https://doi.org/10.1021/acs.cgd.8b01799.

(32) Mínguez Espallargas, G.; Brammer, L.; Allan, D. R.; Pulham, C. R.; Robertson, N.; Warren, J. E. Noncovalent Interactions under Extreme Conditions: High-Pressure and Low-Temperature Diffraction Studies of the Isostructural Metal−Organic Networks (4-Chloropyridinium)2[CoX4] (X = Cl, Br). *J. Am. Chem. Soc.* **2008**, *130* (28), 9058–9071. https://doi.org/10.1021/ja8010868.

(33) Madsen, S. R.; Lock, N.; Overgaard, J.; Iversen, B. B. Anisotropic Thermal Expansion in a Metal–Organic Framework. *Acta Crystallogr., Sect. B: Struct. Sci., Cryst. Eng. Mater.* **2014**, *70* (3), 595–601. https://doi.org/10.1107/S2052520614003497.

(34) Madsen, S. R.; Moggach, S. A.; Overgaard, J.; Brummerstedt Iversen, B. Anisotropic Compressibility of the Coordination Polymer Emim[Mn(Btc)]. *Acta Crystallogr., Sect. B: Struct. Sci., Cryst. Eng. Mater.* **2016**, *72* (3), 389–394. https://doi.org/10.1107/S2052520616005515.